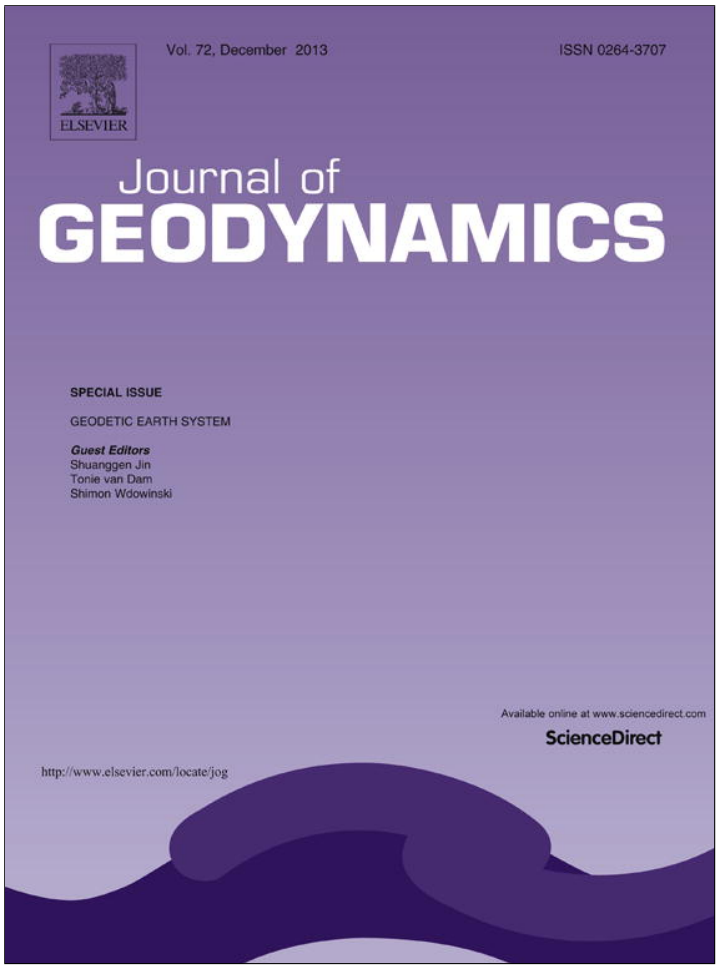

Journal of Geodynamics 72 (2013) 11–24

Contents lists available at ScienceDirect

Journal of Geodynamics

journal homepage: http://www.elsevier.com/locate/jog

Terrestrial reference frame NA12 for crustal deformation studies in North America

Geoffrey Blewitt*, Corné Kreemer, William C. Hammond, Jay M. Goldfarb

Nevada Bureau of Mines & Geology, and Nevada Seismological Laboratory, University of Nevada, 1664N. Virginia St., MS 178, Reno, NV 89557, USA

ARTICLE INFO

Article history:
Received 11 May 2013
Received in revised form 8 August 2013
Accepted 10 August 2013
Available online 28 August 2013

Keywords:
Geodesy
Tectonics
GPS
Reference frame
North America
Deformation

ABSTRACT

We have developed a terrestrial reference frame for geodetic studies of crustal deformation in North America. This plate-fixed frame, designated NA12, is based on GPS data from 1996.0 to 2012.1. Time series of daily coordinates in NA12 for over 5000 GPS stations are updated every week and made publicly available. NA12 is a secular frame defined by 6 Cartesian coordinates of epoch position and velocity of each of 299 stations selected by specific quality criteria, with step-free time spans of 4.7 to 16.1 years (mean 8.8 years). NA12 is aligned in origin and scale with IGS08, a GPS-based realization of global secular frame ITRF2008, so that vertical motion is with respect to the Earth-system center of mass to ±0.5 mm/yr. NA12 is designed to have no-net rotation with respect to the stable interior of the North America tectonic plate, realized by a 30-station core subset. For data after 2012.1, the 299 frame stations have a daily RMS scatter about their frame-predicted positions of 1.0 mm in the north, 0.9 mm east, and 3.4 mm vertical. The 30 core stations have an RMS velocity about zero of 0.2 mm/yr in the north, and 0.3 mm/yr east, some fraction of which results from far-field post-glacial rebound. Given that core station selection was independent of the stations' horizontal velocity, we find unbiased evidence that the North America plate interior is rigid to 0.3 mm/yr. The accuracy of relative horizontal velocities spanning 2000 km are also at a similar level. The rotation of NA12 agrees well with the ITRF2008 plate motion model, but differs from frame SNARF1.0 by 4.2° in the longitude of the North America Euler pole due to far-field post-glacial rebound modeled in SNARF. Just as with ITRF, the NA series of reference frames will need to be updated every few years to mitigate degradation of the frame with time.

1. Introduction

Geodetic GPS techniques can produce station coordinate time series with few millimeter precision, and can produce velocities that sample the movement of the Earth's crust over many years to within a few tenths of a millimeter per year (e.g., Blewitt, 2007). To be reproducible and comparable over long time scales, station positions and velocities must be measured in some well-defined, stable frame of reference. A stable secular reference frame is one in which a linear motion model predicts station positions with sufficient accuracy within a spatial and temporal window of interest. In geodesy, a secular terrestrial frame of reference is realized by a selected set of "frame stations" firmly attached to the solid Earth, whose positions are defined by a set of Cartesian coordinates of position at a conventional epoch, and a corresponding set of velocity coordinates, as described by the IERS Conventions (Petit and Luzum, 2010).

So the task of developing a frame amounts to selecting the frame stations and defining these epoch position and velocity coordinates, which in turn are derived from geodetic observations. The process of defining a unique set of positions and velocities from observations at these selected frame stations requires that certain choices be made to fix the frame. These choices may have physical significance. For example, a natural frame of reference in which to describe station motion driven by plate boundary deformation has its coordinate axes fixed with the stable part of the plate, rotating with the plate, and free from the effects of plate boundary stresses. We call this a "plate-fixed frame".

Other choices may be purely conventional and have no physical significance, but are mathematically necessary to define a unique set of coordinates. Whether the choices be physical or conventional, a convenient approach is to align certain aspects of the new frame with an existing frame that is already broadly used. We call this a "derivative frame." Aspects of a secular derivative frame that can be aligned (or be aligned differently) with an existing frame include 14 transformation parameters: scale, orientation vector, origin vector, scale rate, rotation rate vector, and translation rate vector (Petit and Luzum, 2010).

* Corresponding author Tel.: +1 775 224 0999.
E-mail address: gblewitt@unr.edu (G. Blewitt).

0264-3707/$ – see front matter © 2013 Elsevier Ltd. All rights reserved.
http://dx.doi.org/10.1016/j.jog.2013.08.004

Here we detail the development of a terrestrial reference frame attached both to the North America tectonic plate and to the Earth's center of mass. Such a frame of reference is designed to facilitate physical interpretation of station velocities, for example, in the search for small signals that could indicate earthquake potential in the continental interior; in geodynamic studies of mountain building and post-glacial rebound; and in understanding how deformation is accommodated across the broad Pacific—North America plate boundary, and the role of components such as the Colorado Plateau, the Rio Grande Rift, and the Great Basin.

The frame we develop here, "NA12", is aligned in origin and scale with reference frame IGS08 (Rebischung et al., 2012), which in turn is derived from the International Terrestrial Reference Frame ITRF2008 (Altamimi et al., 2011). NA12 differs from ITRF2008 in that (1) NA12 has 299 stations in and around North America, which is far more than ITRF2008 has in this region; (2) NA12 uses GPS observations through early 2012, and (3) the rotation rate of NA12 is fixed to the stable interior of the North America tectonic plate. The geographic domain of the stable plate interior is specified to be far from plate boundaries, and also in the far-field of post-glacial rebound (Calais et al., 2006; Sella et al., 2007), so that stations within this region are not expected to move significantly relative to each other. Velocities of a core subset of frame stations in this region are used to estimate the angular velocity vector of the plate in the global frame, thus fixing the NA12 coordinate axes to co-rotate with the plate. We align all non-rotational aspects of the frame with ITRF2008 so that vertical motion in the frame has the same physical significance. By taking this approach, the derivative frame origin and translation rate aligns with ITRF2008, which realizes the long-term Earth system mean center of mass to within ±0.5 mm/yr (Altamimi et al., 2011).

2. Methods

2.1. GPS data and data processing

GPS data in daily RINEX files from 1996.0 to 2012.1 were processed from all dual-frequency, continuously operating stations in a defined region in and around North America that we could find in various national and regional archives, including CORS-NGS, UNAVCO, CDDIS, SIO, PANGA, and BARD. The region is chosen to be larger than the North American continent so that more distant stations, e.g., from Hawaii, would help stabilize the orientation of the resulting frame. The specific geographic bounds were latitude >15° and 170° <longitude <347°. It was required that receivers and antennas be of a known type, with absolute antenna phase calibrations (Schmid et al., 2007) available from the International GNSS Service (IGS). Approximately 5000 stations were processed in this initial pool of candidate frame stations.

GPS data were processed using the GIPSY OASIS II software made available by the Jet Propulsion Laboratory (JPL), and using JPL's final fiducial-free GPS orbit products (Bertiger et al., 2010). The precise point positioning method was applied to ionospheric-free carrier phase and pseudorange data (Zumberge et al., 1997). Data initially at the 15 or 30 s data intervals were automatically edited using the TurboEdit algorithm, then at 5-min intervals, carrier phase data were decimated and pseudorange carrier-smoothed (Blewitt, 1990).

In general, models were applied as recommended by the International Earth Rotation and Reference Systems Service (IERS) Conventions (Petit and Luzum, 2010). To model tropospheric refractivity, the Global Mapping Function was applied (Boehm et al., 2006), with tropospheric wet zenith delay and horizontal gradients estimated as stochastic random-walk parameters every 5 min (Bar Sever et al., 1998). For the station motion model, ocean loading was computed using coefficients given by the Ocean Tide Loading Provider hosted at Chalmers University (http://holt.oso.chalmers.se/loading; Scherneck, 1991), for which the FES2004 tidal model was applied. Even though the frame of JPL's fiducial-free orbits is loose, orbit dynamics together with the lack of degree-1 gravity coefficients imply that the orbits are nominally centered on the Earth system center of mass (CM); hence for consistency, ocean loading was modeled in the CM frame (Blewitt, 2003; Fu et al., 2011). Finally, ambiguity resolution was applied to double differences of the estimated one-way bias parameters (Blewitt, 1989), using the wide lane and phase bias (WLPB) method, which phase-connects individual stations to IGS stations in common view (Bertiger et al., 2010).

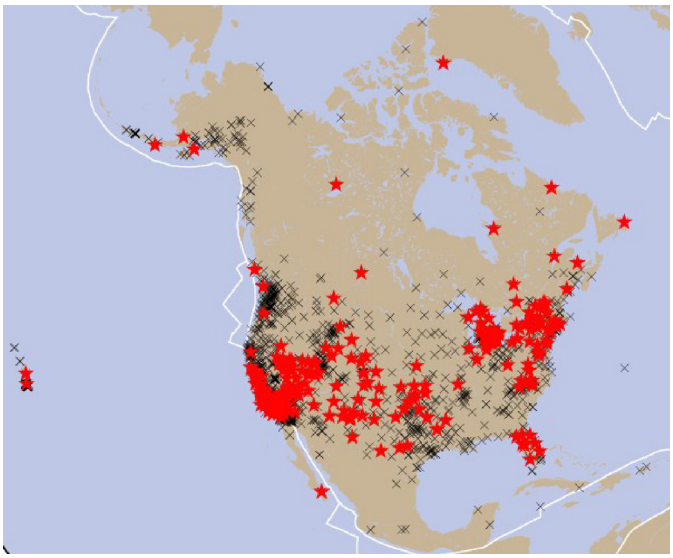

Fig. 1. Frame stations (red stars) selected from candidate stations (black crosses). Plate boundaries are shown in white.

Output station coordinates processed this way are initially in the loose frame of JPL's fiducial-free GPS orbits. These were transformed into reference frame IGS08 using daily 7-parameter transformations that are delivered with JPL's orbit products. IGS08 is a frame that is derived from ITRF2008 and consists of 232 globally distributed IGS stations (Rebischung et al., 2012).

The data processing system includes quality control, such as iterative outlier detection of the input observations, and rejecting output coordinates if the data fail to meet certain criteria such as number of unresolved cycle slips, fraction of the day spanned by the data, and formal errors. Only stations with output coordinate time series spanning at least 5.5 years were accepted as provisional candidates for frame stations, since this minimizes the bias associated with seasonal signals (Blewitt and Lavallée, 2002). This resulted in 1574 provisional candidate frame stations shown in Fig. 1.

2.2. Frame station selection

As NA12 is a secular frame, frame stations were selected based on how well their motions can be described by a constant velocity, at least over segments of data that span at least 4.5 years (Blewitt and Lavallée, 2002). Characteristics of GPS coordinate time series that were used to make this decision included the detection of steps in the time series (whether by earthquake, equipment change, or unknown reasons), the assessment of data quality in terms of residual variance, slow non-linearity, and seasonal signals.

As a first step, the 1574 provisional candidate station time series were subjected to a series of objective selection criteria: (1) the time series must have segments of data spanning at least 4.5 years

(within the provisional minimum of 5.5 years) with no significant steps detected by an automatic step-detection algorithm; (2) the time series must have an RMS coordinate scatter smaller than 2.0 mm east, 2.0 mm north, and 6.4 mm up; (3) the time series must have an estimated annual sinusoidal amplitude smaller than 1.2 mm east, 1.3 mm north, and 3.6 mm up. Not only do these amplitude criteria minimize bias in rate estimation in the presence of seasonal signals (Blewitt and Lavallée, 2002), they also guard against selecting sites on unstable ground subject to local seasonal hydrological deformation that are likely to have more general non-linear variation.

The automatic step detection algorithm is described in Appendix A and is briefly described here. Before executing the algorithm, step magnitudes are estimated at all epochs for which equipment-related discontinuities are likely, as indicated when IGS logs are available. The algorithm first searches for a likely epoch for a single (additional) step. The epoch is chosen as that which minimizes the quadratic form of the residuals (chi-squared statistic). Next, with this epoch held fixed, a second step epoch is found using the same criterion. This process is repeated, until either the estimated magnitude of the final step is below an arbitrary threshold or until a preset maximum number of steps is reached. At each iteration all basic station motion parameters and step magnitudes are re-estimated, as is necessary in such non-orthogonal models. It should be noted that the method as described overestimates the number of steps in a series. Very small steps were provisionally flagged rather than being a cause for immediate rejection, and were manually screened in the next step.

Applying these selection criteria resulted in 378 remaining candidate frame stations. Further manual screening weeded out 79 stations with visibly suspect behavior, leaving a final total of 299 frame stations (Fig. 1), the vast majority spanning >5.5 years, with only 8 stations spanning between 4.5 and 5.5 years. Due to detected steps in most of the time series, stations have a time window of validity, meaning that their data are not to be used to define the frame outside a specified time window.

An alternative approach could have been to estimate steps while assuming a constant velocity. We chose our approach of selecting the longest linear segment because (1) it is simpler and makes less assumptions; (2) change in velocity or non-linear behavior can be associated with steps, for example when equipment is failing and is changed, when radomes are installed and change the antenna gain at lower elevations, or when earthquakes occur; (3) longer segments are longer (and safer) to test for non-linearity; and (4) we have the luxury of having more than enough stations without having to expose ourselves to potential systematic bias arising from assumptions on velocity.

A histogram (Fig. 2) of time spanned by step-free data for the selected frame stations peaks at 5–7 years, and steadily declines to 16 years, with a secondary peak at 10–12 years. This secondary peak appears to be caused by a number of factors, including a spurt of station installation, the M_W7.1 Hector Mine earthquake of October 16, 1999 and subsequent post-seismic relaxation which caused truncation of long time series in a cluster of stations in southern California, and the installation of SCIGN radomes at many western US stations during 1999 and 2000.

There are 8 stations spanning the maximum of 16.1 years that are not fit with any steps, including ALGO, CHIL, CIT1, HBRK, LEEP, NEAH, ROCK, and STJO. There were equipment changes and very small steps indicated at some of these stations, but their long time span overwhelms any problems with systematic error in velocity if very small steps exist. These 8 stations provide a kind of primary backbone that helps hold the frame together in time, as well as being essential to provide a frame during 1996.

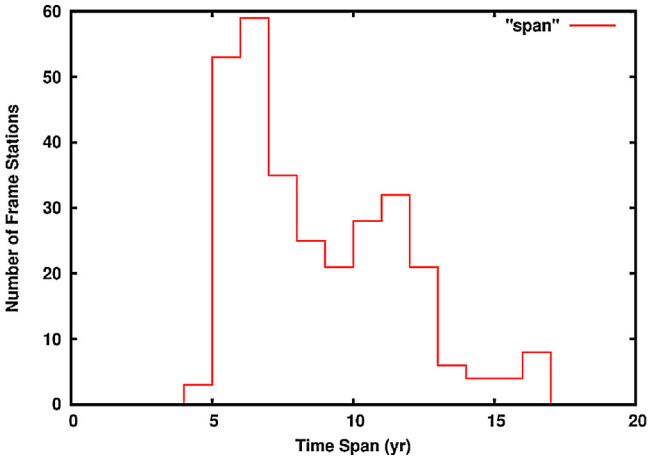

Fig. 2. Histogram of number of frame stations versus time span of step-free data.

2.3. Core station selection

The rotation rate of NA12 is defined with the intention that points within a geographical domain representing the "stable North America plate interior" are not expected to move significantly horizontally. Plate boundary deformation to the west limits this stable domain somewhere to the east of the Basin and Range Province and the Rio Grande Rift (e.g., Kreemer et al., 2010a; Berglund et al., 2012). Horizontal deformation driven by post-glacial rebound centered around Hudson Bay theoretically peaks around the nodal contour of vertical motion (e.g., Sella et al., 2007; Calais et al., 2006), thus further limiting the stable domain farther south than the US-Canadian border. We chose a domain bounded to the west by longitude $\leq$104.6°W and to the north by latitude <40.2°N, which is sufficiently large ($\sim$2000 km), while bounding expected variations in horizontal velocities to <0.5 mm/yr for stations firmly attached to the Earth's crust.

The core stations were required to have vertical velocity magnitudes <0.8 mm/yr to guard against non-tectonic motions such as post-glacial rebound and hydrological effects at stations not firmly attached to the Earth's crust. Constraints were not placed on horizontal velocities so that, in the end, accuracy could be assessed without bias. Of the 299 frame stations broadly distributed around North America, this procedure resulted in a subset of 30 "core stations", which were then used to impose the no-net rotation condition (Fig. 3).

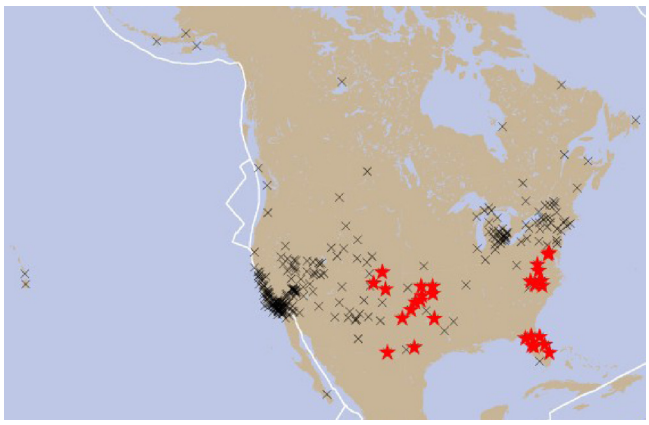

Fig. 3. Core stations (red stars) selected from frame stations (black crosses).

2.4. Continental-scale spatial filtering

Another aspect of the development of the NA12 frame is a more generalized application of spatial filtering (Wdowinski et al., 1997) to improve the resolution of geophysical signals in the GPS station coordinate time series. With the NA12 reference frame defined, the frame station coordinates can be predicted at any point in time. By comparing GPS estimates of frame station positions (in the frame of the GPS orbits) with the frame-predicted positions on any given day, a 7-parameter similarity transformation (origin vector, orientation vector, and scale) can be estimated for that day (Blewitt et al., 1992). This similarity transformation can then be applied to the estimated positions of any station in the region of North America to compute its coordinates in NA12. In addition to expressing the station position in a plate-fixed frame, this effectively applies a continental-scale spatial filter to the station coordinate time series, which is designed to reduce common-mode errors, hence sharpening the signal-to-noise ratio of geophysical effects in the time series for processes smaller than the continental scale.

2.5. Frame construction

On each day, each station has a precise point position solution file with 3 Cartesian coordinates, and a 3×3 covariance matrix. No inter-station correlations can be computed in the precise point positioning technique itself, as each station's data are processed independently. As will be detailed below, we address this deficiency when fitting station velocities by using a full network weight matrix that models inter-station correlations resulting from a 7-parameter common-mode daily transformation (Blewitt, 1998). Frame construction, the most technical aspect of our methodology, was conducted in an iterative manner using these daily coordinate data from the 299 frame stations in their time windows of validity.

The procedure described in the next paragraph was executed three times, with each cycle deleting outlier coordinates with iteratively tighter constraints. The first iteration simply removed gross outliers (15 mm horizontal, 35 mm vertical) and coordinates with large formal errors (4.3 mm horizontal, 12 mm vertical). The second iteration removed course outliers (5 standard deviations). The third iteration implemented spatial filtering (as described in Section 2.4), together with a finer detection of outliers (4 standard deviations), using the previous step's velocity solution as an interim reference frame. One final fourth step captured any remaining finer-scaled outliers.

First, on each day, individual precise point position solutions were concatenated into a single network solution with a block-diagonal covariance matrix. The covariance matrix was then augmented or "loosened" assuming large variances in the 7 transformation parameters using procedure described by Blewitt (1998). This covariance augmentation is accomplished using the (little-known) GIPSY OASIS II command "staproject-u". The resulting full covariance matrix is then suitable to invert into a full weight matrix to be used for a global fit to all station epoch positions and velocities in one step. Seasonal signals and steps were not estimated when constructing the frame, because frame stations were already selected to have small annual signals and no steps over time windows of at least 4.5 years (Blewitt and Lavallée, 2002).

Mathematically, this covariance augmentation procedure was shown by Blewitt (1998) to be equivalent to estimating a daily 7-parameter transformation simultaneously with the velocities and epoch positions, thus minimizing bias in the solution from the internal constraints imposed by the parent frame, IGS08. The idea is to connect to IGS08 (hence ITRF2008) only at the external level, where it is needed to connect to the Earth center of mass. The internal geometry of NA12 is therefore negligibly biased by possible discrepancies between IGS08 and NA12.

The final solution for frame station velocities was then rotated to minimize residual velocities for the 30 core stations. The final covariance matrix was projected onto residual space (Blewitt et al., 1992), and output as a block diagonal matrix, with no inter-station correlations, which is consistent with the original precise point position block structure. The variances were scaled by the overall chi-square per degree of freedom so that formal velocity errors are consistent with the scatter of the data about the constant velocity model.

3. Results and discussion

3.1. Station epoch position and velocity coordinates

Table B1 shows the resulting NA12 frame parameters for the 299 frame stations, including station names, station position Cartesian coordinates referenced to epoch 2005.0, velocity Cartesian coordinates, start and stop epochs, and time span of step-free data. In general, the start and stop epochs define the window of validity. Users of the NA12 frame parameters should be aware that they only apply within the window of validity. The exception to that rule is the latest stop epoch of 2012:049 (year:day), which corresponds the date of last data contributing to the frame. That is, the 239 stations with a stop epoch of 2012:049 continue to be used to extrapolate the frame beyond that end date.

3.2. Plate stability and internal accuracy of the frame

The horizontal velocities of the 30 cores stations, shown in Fig. 4, are not significantly different than zero at the 95% confidence level. The resulting RMS velocity of the core stations is 0.2 mm/yr in the north, and 0.3 mm/yr east, some of which may result from far-field post-glacial rebound. Given that core station selection was independent of the stations' horizontal velocity, this indicates that the North America plate interior is rigid at the level of 0.3 mm/yr, and that relative horizontal velocities over 2000 km have been determined by GPS with a similar level of accuracy.

Frame stations outside the core region show non-zero velocities with patterns that correlate with geographic region (Fig. 5). In the northeast US and across the border into Canada, stations tend to move in a southward direction, which is away from Hudson Bay, the center of post-glacial rebound. To the west of the Rockies in the US, stations in the Great Basin are seen to move increasingly westward in the direction of extension in the Basin and Range Province.

3.3. North America—Pacific plate rotation

As shown in Fig. 6, the northwest motion of the Pacific plate approximately parallel to the plate boundary transform is evident, providing a first-order accuracy check on the physical alignment of the frame. Station MIG1, for which we have 13 years of data, lies on San Miguel Island, and is the station farthest into the Pacific plate away from the plate transform boundary in California. Results from MIG1 give a velocity of 46.6 mm/yr with azimuth -40.6° clockwise from north. NA12 results for MIG1 are shown alongside the predicted Pacific—North America plate motion from three global plate tectonic models in Fig. 7, including NUVEL-1A (DeMets et al., 1994), GEODVEL (Argus et al., 2010), and MORVEL (DeMets et al., 2010). The NA12 velocity for MIG1 agrees with all models of Pacific—North America plate motion to within a similar level of discrepancy as between the models themselves. The agreement is best in speed with model NUVEL-1A, and in azimuth with model GEODVEL. In all four cases, the velocity direction of the Pacific Plate as represented by MIG1 is closely aligned with the trace of the San Andreas Fault in its creeping central section north of the Big Bend.

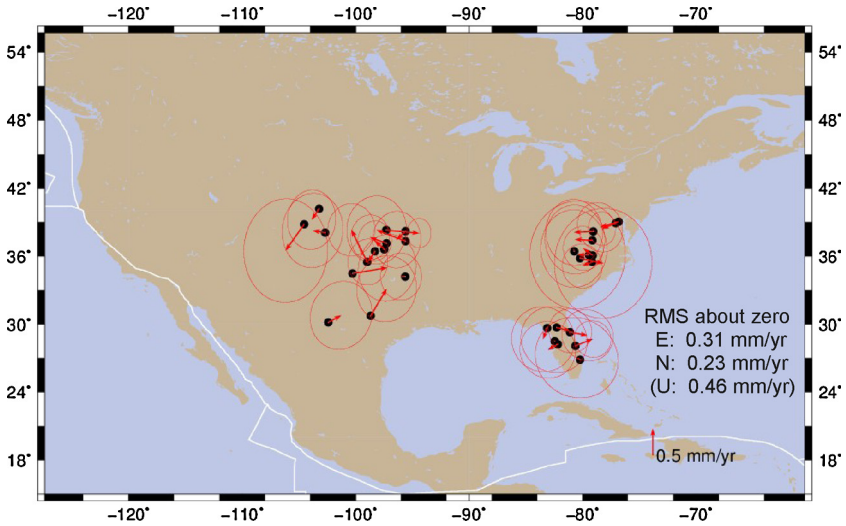

Fig. 4. Core station velocities with 95% confidence ellipses provide an accuracy check.

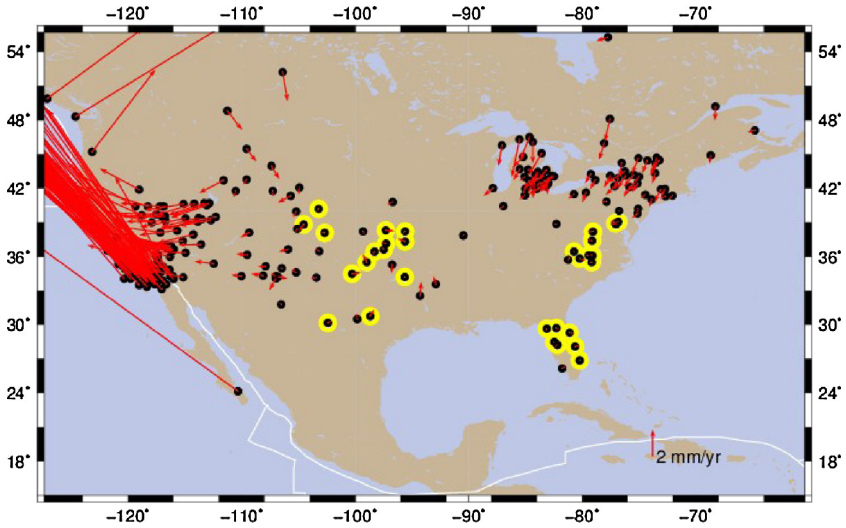

Fig. 5. Assessment of core station selection. Velocities of core stations (with yellow circles) are shown together with other frame stations, indicating the effects of plate boundary deformation in the west, and post-glacial rebound in the northeast. To compare velocity details at core stations versus surrounding stations, some stations have arrows extending beyond the map boundary.

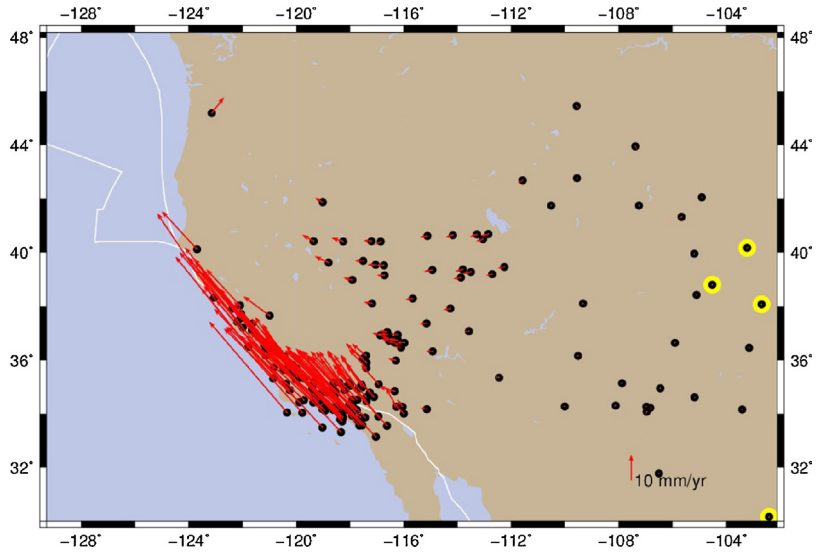

Fig. 6. Alignment of western US station velocities with Pacific—North America transform geometry. Western-most core stations are highlighted by yellow circles.

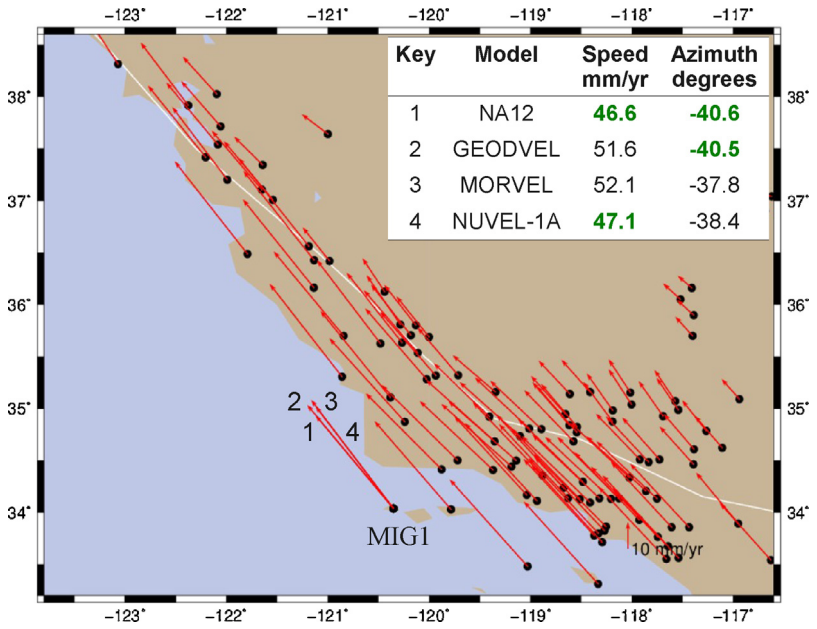

Fig. 7. Zoom in on Pacific—North America plate boundary, showing NA12 frame station velocities. Also shown is a comparison of NA12 with plate tectonic model predictions of Pacific plate velocity. Unlike the geophysical tectonic models, NA12 has no model of the motion of the Pacific plate, which is why the observed velocity of station MIG1 was selected for this comparison. The best agreement is with the azimuth of GEODVEL, and with the speed of NUVEL-1A.

The speed of MIG1 in NA12 is the smallest of all models. This is likely because MIG1 is not entirely in the stable interior of the Pacific plate, which in turn may indicate either nearby offshore activity of the California continental borderlands fault system (McCaffrey, 2005; Meade and Hager, 2005). The Pacific plate itself may not be entirely rigid at a detectable level; e.g., it may be subject to thermal contraction (Kumar and Gordon, 2009; Kreemer et al., 2010b). Another possible explanation is that the differences between the models arise from realizing the no-net rotation condition of the North America plate. Specifically, as discussed in the next section, far-field post-glacial rebound may displace the fitted Euler Pole and affect horizontal velocities in California. All these explanations may apply to some degree.

3.4. North America absolute plate rotation

The angular velocity vector that minimizes the least square residual velocities of the 30 core stations represents the tectonic rotation of the North America plate within IGS08, and hence the ITRF2008 reference frame. We find an angular velocity in Cartesian coordinates of $(0.0042 \pm 0.0004, -0.1741 \pm 0.0020, -0.0305 \pm 0.0014)$ degrees per million years. This corresponds to an absolute Euler pole at $-88.6 \pm 0.1^\circ$ longitude, $-9.9 \pm 0.5^\circ$ latitude, with counter-clockwise rate of rotation of $0.177 \pm 0.002^\circ$/Ma.

Comparing absolute plate rotations with geophysical plate motion models is not straightforward, as plate motion models are inherently relative, and the no-net rotation condition may not correspond to that of ITRF2008. For this reason, care must be taken not to over-interpret the angular velocity and formal errors in geophysical terms. We can however compare our results with the absolute plate rotation estimates derived directly from ITRF2008 station velocities. This also applies to previous versions of ITRF and their derivative frames, to the degree that ITRF realizations are constrained to have the same conventional rotation rate.

Using ITRF2008, Altamimi et al. (2012) estimates a North America Euler pole at $-88.0 \pm 0.7^\circ$ longitude, $-7.9 \pm 0.8^\circ$ latitude, with rate of rotation of $0.184 \pm 0.003^\circ$/Ma. The differences from NA12 are not large statistically. We might expect small systematic differences from the frames having different sets of core stations. For example, the ITRF2008 plate motion model includes stations to the northeast of our defined geographic domain for the stable plate interior for NA12, which are clearly affected by post-glacial rebound (Fig. 5).

We now compare NA12 to the SNARF reference frame, which is the frame currently used by the Plate Boundary Observatory of the NSF EarthScope Program (Herring et al., 2008). SNARF1.0 is a frame aligned with IGb00, hence ITRF2000. SNARF1.0 has a North America Euler pole at $-84.4 \pm 0.3^\circ$ longitude, $-7.4 \pm 0.9^\circ$ latitude, with rate of rotation of $0.188 \pm 0.003^\circ$/Ma. NA12 and SNARF1.0 differ significantly by 4.2° in longitude of the Euler pole. This corresponds closely to the *X*-component of angular velocity, which in turn implies a difference in north–south motion of the core stations.

A major difference between SNARF and other plate-fixed frames such as NA12 and the ITRF2008 plate rotation model, is that SNARF effectively calibrated the observed velocities for the effect of post-glacial rebound, which is modeled at the mm/yr level in the northward direction for core stations. This explains the systematic difference between SNARF and NA12 Euler poles. On the other hand, NA12 proves that the internal deformation in the stable plate interior is negligible, at most 0.3 mm/yr. As shown by Sella et al. (2007) and Peltier and Drummond (2008), models of post-glacial rebound with different layered rheology tend to result in north–south far-field motion in the region of the stable plate interior, but the magnitude and the sign of the motion depends on the specifics of the layered model.

Both frames of reference NA12 and SNARF are valid in that they are based on a rigid plate interior, but users should understand that stations in the plate interior will appear to move in SNARF at the mm/yr level, and not so in NA12. Therefore the velocities of stations in NA12 may be more suitable to study intraplate earthquakes, e.g., New Madrid (Calais et al., 2005), and to interpret how deformation starts to be accommodated when traversing from the stable plate interior into the zone of plate boundary deformation west of the Rio Grande Rift and Wasatch Front. On the other hand, the interpretation of NA12 station velocities far from the stable plate interior, such as in Alaska or Greenland, should consider the relative velocity between that region and the stable plate interior due

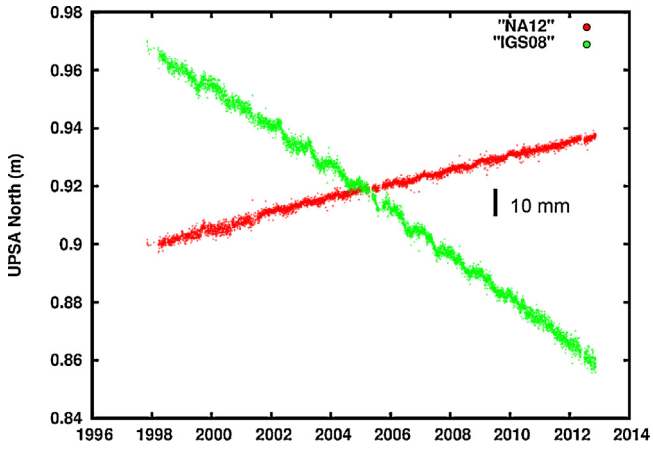

Fig. 8. Example of GPS coordinate time series: North component at station UPSA (Nevada) in both the IGS08 frame and NA12 frame with continental-scale spatial filtering. The scatter of NA12 time series is typically a factor of 2 smaller than in IGS08.

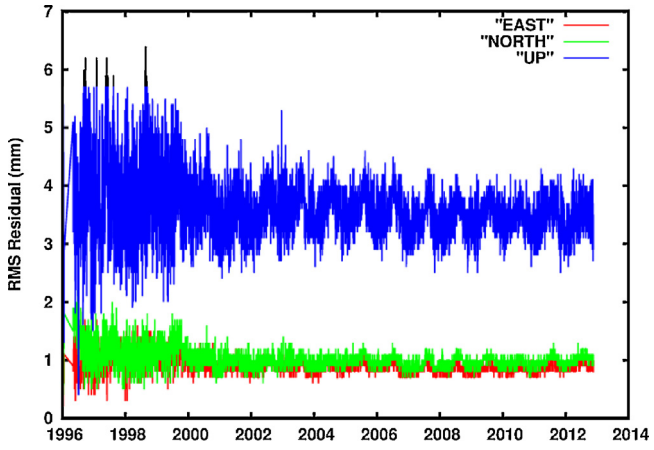

Fig. 10. RMS of observed minus predicted frame-station coordinates versus time. The latest data points are forward-predicted beyond the time window of the frame, and so indicate the level of frame stability, which will eventually degrade with time.

to post-glacial rebound, for which models can differ significantly (Argus and Peltier, 2010).

3.5. Time series precision

Time series for over 5000 stations have been spatially filtered in the NA12 frame, and continue to be updated every week and made publicly available. These time series typically show about a factor of two smaller RMS scatter than time series in IGS08. Typical examples are shown both for horizontal (Fig. 8) and vertical coordinates (Fig. 9). Time series, plots, and transformation parameters are available through http://geodesy.unr.edu.

Since the scatter of time series may be due to real geophysical signals or equipment changes, a more rigorous handle on precision is to use the time series of the frame stations themselves during their window of validity. Since there are 299 frame stations, no one frame station can significantly improve its own results. Seven parameters were computed every day since January 1996 to transform station position coordinates from JPL's orbit frame, into NA12. For each of these daily transformations, residuals were computed between the observed and predicted coordinates on that day. Frame stations are rejected from the daily transformation computation if any observed coordinate lies more than 4 standard deviations away from the predicted position. This precaution is especially important to guard against undetected steps that might occur after the 2012.1, the last date of frame data. The RMS coordinate results are plotted in Fig. 10.

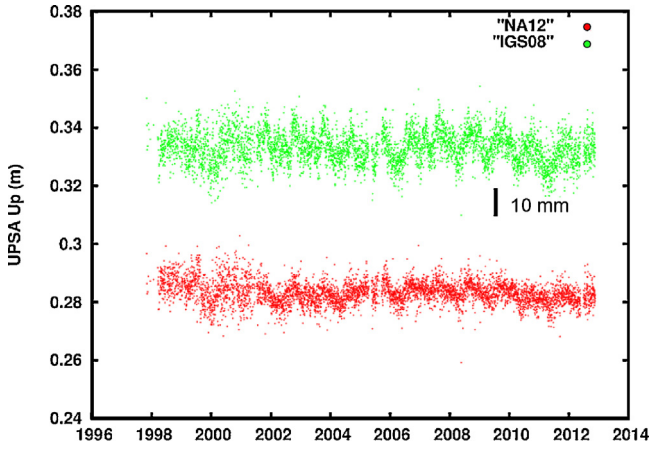

Fig. 9. Example of GPS coordinate time series: up component at station UPSA (Nevada) in both the IGS08 frame and NA12 frame with continental-scale spatial filtering. The scatter of NA12 time series is typically a factor of 2 smaller than in IGS08. The time series have not been detrended. Zero up velocity can be interpreted as no vertical displacement relative to the Earth system center of mass.

The RMS is less stable in earlier years, which is a result of having fewer stations to define the frame, which causes "frame noise". The RMS tends to become more stable with time, and exhibits a small but clearly visible seasonal signal, with the RMS being smaller in the winter and larger in the summer. We interpret this as being due to higher temperatures in summer, which is correlated with increased wet tropospheric delay and its variations. Seasonal variation in non-tidal loading may also play a role.

For data after 2012.1, which is beyond the window of data used to define the frame, the RMS coordinate residuals to the estimated transformation are at the level of 1.0 mm in the north, 0.9 mm east, and 3.4 mm vertical. These parameters can be applied directly by other users of the GIPSY OASIS II software, and are publicly available at ftp://gneiss.nbmg.unr.edu/xfiles. It is important when applying these files that exactly the same orbits and observable models are used, which in this case are the fiducial-free final orbits computed by JPL using the GIPSY OASIS II software with WLPB ambiguity resolution applied. Implementation of these published files by non-GIPSY software is therefore not recommended, though a similar scheme could be implemented to estimate transformation parameters specific to each set of software and orbit product.

Transformation parameters are not given for some days (mostly in 1996), because of poor network geometry in earlier years, which we detected by inspection of the formal errors in the transformation parameters. However, by 2000 there were 100 contributing frame stations. During 2012 there are up to ~200 contributing frame stations per day (Fig. 11). The seasonality in contributing stations is due to the effect of increased RMS scatter in the summer season, which in turn tends to reject more contributing stations from the transformation computation.

As stations fail, equipment is replaced, and large earthquakes occur, the number of contributing frame stations naturally tends to decrease with time since 2006.6 (Fig. 11), the latest start date of a frame station (5.5 years prior to 2012.1, the last date of frame data). This factor, together with increasing extrapolation error in the predicted position of frame stations with time, implies that the reference frame starts to degrade as soon as it is built. Frame degradation is a well known phenomenon that can be addressed by serial reference frame updates (e.g., Rebischung et al., 2012). For example, prior to NA12 was a prototype frame, NA09. It is convenient to update the derivative frame whenever the parent frame is updated.

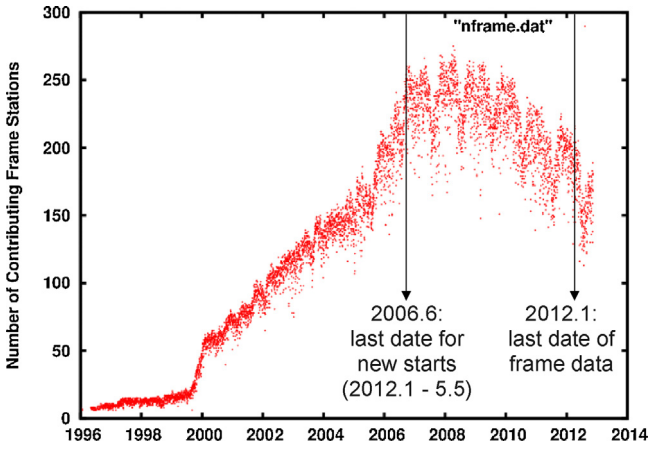

Fig. 11. Number of actively frame stations versus time. Frame stations may be decommissioned or become disqualified to contribute if a step is detected in the time series, eventually leading to frame degradation with time.

Therefore the NA series of frames will be updated when new versions of ITRF and IGS frames become available, though there is also the option of additional updates in between parent frame updates.

4. Summary and conclusions

Designed for geodetic studies of crustal deformation in North America at the sub-millimeter level, NA12 is a secular terrestrial reference frame based on 299 GPS stations required to have data spanning at least 5.5 years from1996.0 to 2012.1, with step-free coordinate time series spanning at least 4.5 years. The step-free time spans have a mean of 8.8 years, and range from 4.7 to 16.1 years. The frame has no-net rotation with respect to the stable interior of the North America plate, and is otherwise consistent with parent frames IGS08 and ITRF2008, so that vertical motions are with respect to the Earth-system center of mass to ±0.5 mm/yr.

Site selection was mainly objective, using an automatic step detection algorithm, and an empirical assessment of statistical quality indicators. Starting with 1578 candidates frame stations, objective criteria reduced the number of 378, after which 299 stations survived a final step of manual screening.

The methodology used to construct the frame involve a simultaneous weighted least squares fit to all frame station data using the technique of covariance augmentation, which effectively loosens the formal variance for linear combinations of data that correspond to frame parameters. Mathematically this procedure implicitly estimates daily transformation parameters simultaneously with station velocities and epoch positions. This method allows the data to define the internal geometry of the frame and its secular evolution in time, while inheriting the external frame geometry (scale, orientation, origin, and their rates) from the parent frame IGS08. Inherent in the frame construction is the spatial filtering of coordinate time series at the continental scale. An iterative procedure is used to remove coordinate outliers and define a spatial filter for the next iteration. As a final step in the frame construction, the no-net rotation condition is realized by 30 core stations selected in the far-field from plate boundary tectonics and post-glacial rebound.

The core station network indicates a relative horizontal velocity accuracy of 0.3 mm/yr, suggesting that the North America plate interior is rigid at this level. The resulting velocities of frame stations offshore California agree in magnitude and azimuth with global plate motion models at the same level as between the various models themselves. The azimuth of all models are consistent that of the creeping central section of the San Andreas fault.

There are statistically small differences between NA12 and the ITRF2008 plate motion model, but we can expect that part of the differences are due to systematic variation in velocity to the north of the core station network in the ITRF2008 model caused by post-glacial rebound. There is ~4° difference in the longitude of the North America Euler pole between NA12 (or ITRF2008) and SNARF1.0 that can be explained by the far-field post-glacial rebound model assumed by SNARF1.0. If such far field deformation is in fact taking place, our results constrain the deformation of the stable plate interior by post-glacial rebound to be <0.3 mm/yr. Although both types of frame are valid, this difference in approach should be considered by users of either frame. Nevertheless, NA12 may be preferred over SNARF1.0 which is now aging considerably.

During 2012, the 299 frame stations have an RMS scatter about their frame-predicted positions of 1.0 mm in the north, 0.9 mm east, and 3.4 mm vertical. Time series of similar precision for over 5000 sites are being updated weekly in the NA12 frame and made publicly available. Daily transformation files are also made publicly available for users of JPL's GIPSY software and fiducial-free orbit products.

Just as with the ITRF and IGS series of reference frames, the NA series will need to be updated in a few years to mitigate degradation of the frame with time. This is largely due to attrition in the number of contributing frame stations, and also due to extrapolation error of frame predicted positions after 2012.1, the last date of frame data. The next update of the NA series will likely be derived from ITRF2013 through IGS13, preparations for which are already underway.

Acknowledgments

We thank Zuheir Altamimi and Eric Calais for their careful reviews that led to improvements to the text. This research was supported by NASA grant NNX09AM74G and NNX12AK26G. We also acknowledge support by NSF grant EAR0844389. Some of the figures have been drawn using Generic Mapping Tools (Wessel and Smith, 1998).

Appendix A. Step detection algorithm

The step detection algorithm is based on successive estimates of the parameters in the equation

$$x^C(t) = C_1 + C_2 t + a_1 \sin\omega t + a_2 \cos\omega t + s_1 \sin 2\omega t + s_2 \cos 2\omega t + \sum_{i=1}^{N} d_i H(t - t_1) \quad \text{(A.1)}$$

where $x^C(t)$ is the computed value of one of the coordinates (north, east, up), t is elapsed time from the initial epoch of the series, C_1 is an offset, C_2 is a component of the station velocity, ω is a natural frequency corresponding to a period of one year, and a_1, a_2, s_1, s_2 are amplitudes of annual and semiannual periodic components, respectively, N is the number of steps in the current solution, d_i is the magnitude of step i, t_i is epoch of step i, and H is the Heaviside function. The terms preceding the summation comprise the basic station motion model.

The number of steps N is the sum of both N_e, the number of steps at known antenna change epochs, and N_u, the number of steps at previously undetermined epochs. In general, we first solve (A.1) with all N_e steps included before the algorithm is run.

The algorithm uses a naive search and proceeds as follows:

(1) For all epochs at which a step might be present, Eq. (A.1) is solved (all parameters estimated) for step $i = N_e + 1$ At each of these epochs the parameters are estimated by weighted

least-squares. The epoch chosen for the step is the one that yields the lowest chi-squared statistic $v^T C_x^{-1} v$ where $v = x(t) - x^C(t)$ is the vector of residual differences between the coordinate value in the original series $x(t)$ and the computed coordinate values computed by (A.1) and C_x is the covariance matrix for $x(t)$.

(2) For step $i = N_e + 2$, $i = N_e + 3 \ldots$, the search described in the previous step is repeated, with the epochs fixed for all previously estimated steps, with the new step epoch chosen based on the same minimization criterion. All parameters in Eq. (A.1) must be re-estimated in each least-squares solution as they are not an orthogonal set. The algorithm stops when either (a) the estimated magnitude of the current step is below a predetermined value, usually two or three times the average formal precision of the values in the series, or (b) a preset maximum number of steps to be estimated has been reached. For example, for a series spanning 10 years this preset maximum might be set to 20.

Note that it is extremely unlikely that there would be 20 actual discontinuities in such a series spanning 10 years. Consequently, subsequent to application of the algorithm, other criteria are often needed to winnow the steps down to a more reasonable number. Criteria which we applied include the F-test statistic (Koch, 1999), the Akaike information-theoretical criterion (Akaike, 1974), and a heuristic based on fitting an arctangent function to steps to quantify their abruptness.

Appendix B. Resulting NA12 frame parameters

Table B1
NA12 reference frame parameters for 299 frame stations, including 30 *core stations.

Station	Position at epoch 2005.0 (m)			Velocity (mm/a)			Start epoch (year:day)	Stop epoch (year:day)	Span (yr)
*Core	X	Y	Z	X	Y	Z			
AB07	−342,5750.0177	−1214,685.9349	5223,662.8319	0.3248	6.5673	1.4428	2004:297	2012:049	7.3
AC24	−3051,338.4784	−1317,097.7992	5425,614.2969	−3.3631	−2.2604	0.0165	2006:182	2012:049	5.6
AC39	−2951,218.9077	−1543,248.7378	5421,552.8393	−8.9990	−6.5473	5.7117	2006:164	2012:049	5.7
ADRI	494,838.2173	−4727,340.1209	4239,050.3246	−0.6539	0.7157	−1.2474	2002:101	2012:049	9.9
ALAM	−2158,287.5048	−4595,239.5546	3849,706.7442	−2.4039	1.1279	−0.2776	1999:355	2010:311	10.9
ALGO	918,129.3735	−4346,071.2655	4561,977.8580	0.2875	−3.2676	1.5866	1996:001	2012:049	16.1
*AMC2	−1248,596.1975	−4819,428.2253	3976,506.0005	−0.3344	0.0875	−0.6305	2002:185	2007:274	5.2
APEX	−2169,121.1084	−4666,190.6867	3757,231.6561	−2.3867	0.7913	0.2830	2000:001	2009:174	9.5
ARCM	−267,628.1573	−5314759.4245	3504,269.3898	−0.1628	0.9807	0.0656	2005:221	2012:049	6.5
ARGU	−2386,308.6827	−4579,773.0478	373,3733.8244	−4.1970	6.3624	4.6102	2000:120	2011:205	11.2
AUBN	413,289.7318	−4776,162.5575	4193,173.5348	−0.4492	0.4503	−0.8142	2003:339	2010:059	6.2
AVCA	594,062.1199	−4629,522.4572	4332,585.3838	−0.5820	0.2300	−1.2319	2003:100	2012:049	8.9
AZRY	−2385,740.3266	−4758,052.1527	3504,739.0087	−12.4960	19.2149	18.1876	2000:001	2010:035	10.1
BAIE	1546,823.2999	−3879,765.1381	4804,185.0649	1.0731	−2.7603	1.8404	2003:063	2012:049	9.0
BAMO	−2223,891.4094	−4326,376.6483	4114,149.9517	−2.7124	1.2024	0.4547	2003:033	2012:049	9.0
BAR1	−2584,162.9637	−4656,252.9081	3498,534.1855	−17.4005	31.0169	27.1353	2006:258	2012:049	5.4
BAYR	493,530.0623	−4611,778.1478	4363,728.8724	−0.5407	0.0615	−1.3519	2001:244	2012:049	10.5
BCWR	−2571,120.4512	−4561,914.8888	3631,398.2186	−13.4156	20.1612	16.9375	2002:037	2012:049	10.0
BEAT	−2284,553.4347	−4557,948.9653	3821,772.3259	−2.3739	1.7233	0.3058	1999:336	2010:238	10.7
BEMT	−2320,746.1195	−4758,616.1230	3547,263.8228	−2.9393	4.3589	3.7655	2001:319	2010:093	8.4
BIGR	363,496.5090	−4606,053.6037	4382,574.7901	−0.4902	0.2639	−1.4230	2006:260	2012:049	5.4
*BKVL	736,863.6932	−5562,275.7349	3022,761.8157	−0.0177	0.0465	0.0075	2003:225	2012:049	8.5
BLW2	−1570,409.8893	−4420,523.2286	4310,050.3128	−0.0331	0.6932	−1.1077	2003:246	2012:049	8.5
BMHL	−2318,199.6976	−4741,880.6759	3569,942.0612	−1.4055	1.7100	2.7062	1999:352	2012:049	12.2
BRCH	497,093.2027	−4626,394.9751	4347,946.1812	−0.5584	0.6812	−1.4434	2004:182	2012:049	7.6
BRIG	512,038.6351	−4680,414.9109	4288,537.4365	−0.2474	0.0758	−0.4972	2001:244	2012:049	10.5
BRPK	−2512,215.7420	−4612,171.0317	3609,922.4298	−11.6828	18.4880	16.1527	2000:342	2012:049	11.2
BULL	−2308,136.9402	−4555,161.2774	3810,897.6563	−2.4754	1.9692	0.7202	1999:336	2011:103	11.4
BUST	−227,9604.7375	−4582,000.4551	3795,378.5263	−2.3731	1.6595	0.2975	1999:336	2010:024	10.1
BVPP	−2558,594.8428	−4550,517.5759	3652,217.0035	−10.2858	15.5888	10.9477	2002:033	2012:049	10.0
CASS	550,879.5835	−4593,314.7629	4376,306.9310	−0.5674	0.0272	−1.1429	2003:100	2011:335	8.6
CAT2	−2532,493.6909	−4696,708.6317	3483,154.2511	−16.8566	29.5312	25.5049	2000:166	2012:049	11.7
CBHS	−2532,244.1907	−4638,721.4926	3559,337.8975	−16.1448	26.5755	23.2494	1999:048	2012:049	13.0
CCST	−2543,426.4366	−4585,920.6511	3621,149.9108	−13.2456	19.6186	16.1139	2003:205	2012:027	8.5
CDMT	−2325,536.3418	−4697,945.8145	3622,888.4066	−5.5103	2.6790	2.2814	2000:292	2010:094	9.5
CDVV	−1540,686.3196	−5048,882.9257	3570,657.2777	−1.0617	−2.1340	1.8242	2005:322	2012:049	6.3
CEDA	−1882,186.3662	−4464,346.9477	4136,557.1105	−2.9181	0.0775	−0.2729	1996:197	2012:049	15.6
CHIL	−2478,003.2467	−4655,349.0872	3577,932.2668	−14.7500	21.0746	17.2058	1996:001	2012:049	16.1
CHSN	476,931.0423	−4633,179.9745	4343,017.6187	−0.2196	0.1952	−2.6040	2005:048	2012:049	7.0
CIRX	−255,8057.3051	−4626,792.2261	3556,788.2744	−16.3998	28.2928	24.2122	2000:293	2012:049	11.3
CIT1	−2491,490.1601	−4660,803.2999	3559,128.9589	−15.5002	21.7751	19.9337	1996:001	2012:049	16.1
CMOD	−2604,474.7276	−4334,577.9500	3874,014.6302	−6.0741	9.5169	5.5608	2004:124	2012:049	7.8
CNPP	−2457,276.1390	−4698,554.3133	3533,511.0440	−14.3191	23.2061	20.3951	2000:050	2012:049	12.0
CONO	790,310.0295	−5124,962.6661	3701,605.0596	0.1132	0.3808	0.0228	2002:275	2010:090	7.5
COPR	−2624,084.9650	−4567,199.8821	3584,495.7618	−17.6755	28.3390	24.1290	2001:180	2012:049	10.6
CPBN	−2419,255.1271	−4632,919.9593	3644,863.3798	−3.6026	10.3466	9.0285	2006:127	2012:049	5.8
CRAT	−2287,201.7038	−4573,564.8280	3800,907.9979	−2.4378	1.4224	0.6139	1999:336	2010:024	10.1
CRHS	−2512,420.0195	−4671,388.5683	3530,186.4521	−16.7224	26.2034	23.4551	2000:299	2006:220	5.8
CRU1	−2628,780.9047	−4592,933.3305	3549,529.6893	−16.3192	31.2845	27.4637	2000:162	2012:049	11.7
CSCI	−2564,318.6062	−4618,739.9940	3561,957.2700	−16.3089	28.4735	24.4792	2000:344	2012:049	11.2
CSDH	−2510,006.5820	−4670,036.4566	3533,692.8119	−18.0495	25.8026	23.6538	1998:191	2012:049	13.6

Table B1 (*Continued*)

Station	Position at epoch 2005.0 (m)			Velocity (mm/a)			Start epoch (year:day)	Stop epoch (year:day)	Span (yr)
*Core	*X*	*Y*	*Z*	*X*	*Y*	*Z*			
CSST	−2583,750.8358	−4590,804.0372	3583,976.6284	−17.2394	27.3585	21.0722	2000:351	2012:049	11.2
CTEG	1413,425.9137	−4537,669.7501	4239,299.8705	−0.3329	0.0683	−0.9217	2005:176	2012:049	6.7
CTGR	1478,106.9637	−4562,612.6823	4190,441.8232	−0.4652	0.7459	−1.0881	2005:176	2012:049	6.7
CTGU	1429,796.9052	−4581,508.3747	4186,611.7860	−0.4887	0.1191	−0.5011	2005:176	2012:049	6.7
CTWI	1384,615.4389	−4548,661.0557	4237,285.4588	−0.3338	−0.5791	−0.8777	2005:175	2012:049	6.7
DET1	568,024.6230	−4690,674.6413	4270,188.8306	−0.0295	0.4363	−1.3858	1996:245	2007:318	11.2
*DOBS	828,618.8790	−5071,130.9137	3766,480.8567	−0.0245	0.0919	−0.0082	2003:120	2010:078	6.9
ECHO	−2070,970.2418	−4594,332.3784	3899,086.7082	−2.4263	1.0706	−0.7534	2000:001	2012:049	12.1
EGAN	−2083,234.2119	−4479,986.3395	4023,297.9434	−2.9142	1.7346	−1.1061	1997:084	2012:049	14.9
ELIZ	−2485,778.2776	−3284,087.0925	4853,826.8518	7.6097	−1.8138	4.4226	2004:201	2012:049	7.6
ESCU	1852,954.5316	−3937,498.7725	4647,314.6642	−0.6530	0.0956	−0.5838	2004:345	2012:049	7.2
FERN	−1989,985.6863	−4815,005.7642	3669,893.7488	−1.0615	1.1743	−0.2571	1999:357	2012:049	12.2
FMVT	−2546,367.0195	−4615,776.2017	3579,494.9727	−15.7578	27.4113	22.3106	2000:335	2012:049	11.2
FOOT	−1993,377.5621	−4518,444.3797	4025,085.9685	−2.6315	0.9280	−0.6348	1999:235	2012:049	12.5
FRTG	610,411.7464	−4629,148.4003	4330,660.0768	−0.7649	0.2661	−0.9749	2003:100	2012:049	8.9
FZHS	−2533,877.2802	−4591,364.6205	3620,414.1072	−12.8424	17.9950	15.7211	1998:214	2012:049	13.5
GABB	−2325,277.9913	−4388,649.4657	3990,731.9331	−2.9684	1.6961	1.0186	1999:352	2010:344	11.0
GALP	668,399.8514	−4929,212.7120	3978,967.6316	−0.2723	0.8829	−0.7668	2003:003	2012:049	9.1
GARL	−2384,509.0416	−4239,524.9305	4114,370.6134	−2.9819	3.5903	1.8058	1996:239	2012:049	15.5
*GNVL	745,247.2486	−5495,263.1035	3140,246.6163	0.2518	0.0298	−0.0695	2002:141	2012:049	9.7
*GODZ	1130,773.7464	−4831,253.5662	3994,200.4212	−0.4409	0.3736	−0.5050	2002:161	2012:049	9.7
GOSH	−1985,697.1441	−4422,567.1540	4133,199.5030	−2.7377	0.7654	−0.7245	1999:213	2012:049	12.6
GUST	772,251.5800	−4724,227.2370	4201,259.6684	−0.5215	0.6257	−1.0758	2006:001	2012:049	6.1
*HBRK	−636,268.6255	−4971,311.1927	3932,291.5344	0.5734	−0.3499	0.1413	1996:001	2012:049	16.1
*HILB	976,016.9061	−5069,590.5658	3733,033.6381	−0.2930	0.5855	−0.2951	2002:100	2012:049	9.9
HURR	−2038,303.6192	−4671,107.0010	3823,609.0081	−1.2717	1.2847	−0.5337	2005:261	2011:334	6.2
HVYS	−2568,089.5000	−4597,402.5437	3587,128.7654	−16.9599	25.5791	19.1142	2000:209	2012:049	11.6
IDSS	−1727,847.5976	−4367,635.2957	4303,180.2203	−1.4788	1.2195	−1.8170	2004:331	2012:049	7.2
IMPS	−2245,206.2722	−4783,197.4109	3561,238.8905	−1.7307	1.7950	0.0069	2000:258	2010:094	9.6
JCT1	−936,591.7002	−5421,681.3867	3216,577.3798	−0.1793	−0.9207	1.0452	2005:298	2012:049	6.3
JOHN	−2259,718.7909	−4612,855.4621	3769,777.7789	−2.1708	1.4365	0.0955	1999:336	2011:103	11.4
KAR2	176,867.1625	−4744,388.9503	4245,130.9135	−0.7225	0.5950	−1.3370	2005:245	2012:037	6.4
KNGS	1067,510.7811	−4452,412.9109	4425,573.1293	0.1727	−1.4644	−0.0328	2002:164	2012:049	9.7
KUUJ	772,857.5372	−3558,198.7256	5219,095.9111	0.9991	−8.6401	12.0170	2005:216	2010:210	5.0
LAMT	1336,027.8031	−4631,479.3259	4162,860.2088	−0.2036	0.1072	−0.8374	2001:232	2007:365	6.4
LANS	436,837.5554	−4676,403.6835	4301,099.4826	−0.4147	0.3236	−1.2706	2002:103	2012:049	9.9
LEEP	−2507,463.3140	−4652,632.0352	3559,086.7736	−16.5492	24.3447	20.0742	1996:001	2012:049	16.1
LEWI	−2198,662.5516	−4340,957.6515	4114,097.3638	−1.9154	0.5285	−1.2848	1999:239	2012:049	12.5
LFRS	−2515,892.4516	−4650,557.5243	3555,266.5976	−16.6462	25.0473	20.7559	1999:093	2012:049	12.9
LITT	−2268,192.5546	−4587,678.0438	3795,464.7051	−2.2854	1.5202	0.0637	1999:256	2010:024	10.4
LL01	−2457,799.4419	−4654,745.9576	3591,531.5472	−10.1134	16.4071	14.2955	2000:229	2012:049	11.5
LNMT	−2367,549.4857	−4658,701.5274	3646,833.1060	−3.9577	7.2851	5.9247	2000:364	2012:049	11.1
LORS	−2461,265.8580	−4677,290.8213	3558,949.5039	−14.9186	21.9594	17.7003	1999:267	2012:049	12.4
LPAZ	−2022,283.3509	−5461,274.3119	2592,317.1176	−31.5901	25.3904	24.8104	2005:245	2010:131	4.7
LVMS	−2552,869.8043	−4585,907.7262	3614,498.1084	-15.1354	21.1317	17.2446	1999:273	2012:049	12.4
MACC	−42,648.2625	−5042,990.6977	3892,014.7821	0.0994	0.4575	−0.3246	1999:286	2007:192	7.7
MAT2	−2443,204.3712	−4706,039.2505	3533,485.3515	−14.1144	22.5107	19.9861	2000:301	2012:049	11.3
MAUI	−5466,068.8819	−2404,328.0730	2242,127.4410	−4.8100	59.6700	49.4320	1999:001	2012:049	13.1
MERC	−2245,157.7466	−4607,537.6983	3785,494.9791	−2.1556	1.3656	−0.1136	1999:234	2011:058	11.5
METR	552,539.1181	−4663,338.3593	4302,000.2672	−0.4971	0.3765	−0.9187	2001:246	2012:049	10.5
MHCB	−2664,063.7070	−4323,171.9425	3848,361.4763	−6.4340	10.6056	9.0983	1999:252	2012:049	12.4
MICW	415,799.8951	−4733,447.9347	4240,803.0187	−0.2756	1.0644	−1.4826	2006:121	2012:049	5.8
MIDS	526,872.4026	−4638,494.4003	4331,705.0961	−1.1981	0.3822	−1.4832	2005:230	2012:049	6.5
MIDT	574,041.9797	−4678,918.7332	4282,207.5978	−0.6338	0.4408	−1.0195	2005:230	2012:049	6.5
MIG1	−2673,548.1947	−4565,823.3514	3550,037.2308	−16.0103	32.6116	29.1743	2000:169	2012:049	11.7
MIKK	380,882.2725	−4522,014.4753	4467,229.0776	−0.7612	−0.0546	−1.0609	2005:329	2012:049	6.2
MION	401,236.4056	−4655,196.3930	4327,289.1499	−0.4680	1.1057	−1.4821	2005:329	2012:049	6.2
MIWA	570,898.5362	−4653,657.4414	4309,940.6343	−0.3367	−0.1034	−1.0945	2005:329	2012:049	6.2
MLRD	−5475,222.2809	−2491,352.6341	2122,433.1282	−6.1894	59.6798	47.0830	2005:080	2012:049	6.9
MONI	−2227,410.7702	−4425,716.6340	4006,379.0084	−2.6170	1.3272	−0.0721	1999:075	2010:143	11.2
MPLE	422,271.3983	−4605,910.8365	4377,365.6245	0.0979	1.4582	−1.3546	2002:036	2012:049	10.0
NAIN	1671,836.6428	−3103,473.3001	5297,671.2209	0.8913	−1.1215	4.3820	2003:001	2012:049	9.1
NAPL	819,477.2559	−5670,155.7209	2793,845.7292	0.1264	0.8926	−0.2544	2006:137	2012:049	5.8
*NCBU	945,967.5216	−5072,710.6718	3736,507.3651	−0.0826	−0.7193	0.5076	2003:310	2008:366	5.2
*NCLE	878,752.5299	−5103,101.0084	3711,657.5005	0.4362	0.0253	−0.0823	2004:127	2009:059	4.8
*NDS1	−495,849.9299	−5055,714.8335	3844,210.0137	−0.5684	−0.2632	0.5092	2002:001	2009:204	7.6
NEAH	−2415,625.6108	−3498,394.0806	4739,316.8487	10.6507	−4.1760	7.3439	1996:001	2012:049	16.1
NEDR	−564,408.7966	−4804,345.9664	4143,558.0467	−0.2645	0.9869	−1.0639	2003:302	2012:049	8.3
NEWS	−2270,836.6254	−4360,576.0305	4052,314.6870	−3.1716	1.0522	0.5803	1999:235	2012:049	12.5
NHRG	−2563,130.7890	−4597,243.8063	3593,102.9937	−16.6592	24.2371	18.4834	2000:265	2012:049	11.4
NJGC	1260,439.3687	−4743,674.2423	4059,354.1160	−0.5678	0.4756	−0.9448	2003:283	2012:049	8.4
NOR3	505,437.3771	−4483,924.2522	4492,858.2378	−0.8175	−1.3101	−1.0895	2001:246	2012:049	10.5
NRL1	1117,249.1659	−4848,758.6920	3976,821.1957	−0.2152	−0.6472	0.8265	2005:160	2012:049	6.7
NYBH	1160,328.5050	−4594,819.4956	4254,865.0695	−0.3780	−0.1812	−0.8947	2006:112	2012:049	5.8
NYCP	1053,192.7498	−4614,551.1894	4261,277.5914	−0.5575	−0.4508	−0.6173	2006:115	2012:049	5.8
NYET	1297,510.1031	−4391,722.9385	4424,942.9804	0.0264	−1.4987	0.1020	2006:115	2012:049	5.8

Table B1 (*Continued*)

Station	Position at epoch 2005.0 (m)			Velocity (mm/a)			Start epoch (year:day)	Stop epoch (year:day)	Span (yr)
*Core	*X*	*Y*	*Z*	*X*	*Y*	*Z*			
NYHB	907,896.9961	−4604,813.0257	4304,633.5343	−0.3618	−0.0515	−0.9115	2006:112	2012:049	5.8
NYHF	1314,717.2402	−4458,037.9466	4353,290.2419	0.0476	−0.9283	−0.1806	2006:112	2012:049	5.8
NYHM	1209,172.8880	−4511,390.7941	4329,062.7898	−0.7835	−0.3799	−1.3948	2006:112	2012:049	5.8
NYMD	1284,926.9283	−4615,400.1410	4196,499.9205	−0.3838	0.2005	−0.5625	2006:112	2012:049	5.8
NYMX	1103,390.7045	−4503,029.4607	4365,614.5836	−1.0184	−1.3571	−0.1244	2006:112	2012:049	5.8
NYNS	1116,898.7162	−4527,274.2092	4337,213.6521	−0.4008	−0.9535	−0.5127	2006:115	2012:049	5.8
NYON	1211,278.5537	−4556,099.1050	4282,024.1661	−0.2243	−0.7223	−0.3249	2006:112	2012:049	5.8
NYPB	1293,674.7884	−4354,525.4560	4462,210.6193	0.2706	−2.0358	0.6044	2006:112	2012:049	5.8
NYPD	1173,100.1112	−4390,883.4835	4460,037.7833	0.1075	−2.3316	0.6155	2006:114	2012:049	5.8
NYPF	1007,671.5938	−4554,835.1546	4335,145.0693	−0.2791	−0.8674	−0.4613	2006:112	2012:049	5.8
NYRM	1167,416.5806	−4509,906.2269	4342,013.7094	−0.4675	−1.0314	−0.3384	2006:112	2012:049	5.8
NYWL	1064,476.0138	−4557,027.6453	4319,337.3135	−0.1065	−0.7280	−0.5153	2006:112	2012:049	5.8
OEOC	−2471,017.3497	−4697,798.6237	3525,085.2300	−15.9690	25.4448	21.8863	2000:197	2012:049	11.6
OGHS	−2430,835.3929	−4762,197.8561	3466,199.0562	−16.7047	25.3093	22.5958	2000:040	2008:094	8.1
*OKAN	−517,317.2724	−5255,838.1068	3564,455.6495	−0.0841	−0.0499	0.0374	2002:231	2012:049	9.5
*OKCL	−810,882.4731	−5136,263.7767	3681,919.1624	−0.2456	0.3491	0.5200	2002:351	2012:049	9.2
*ORMD	860,375.7586	−5499,831.8283	3102,756.7431	0.3053	0.1647	−0.1348	2003:093	2012:049	8.9
OXYC	−2498,227.9966	−4657,747.8141	3558,400.7887	−16.1743	23.9854	19.1717	1999:285	2012:049	12.4
OZST	−2574,193.7649	−4577,157.2219	3609,640.4579	−17.0875	23.8913	19.6495	2000:320	2012:049	11.3
P011	−1723,275.3480	−4861,194.4398	3742,648.4295	−0.6066	0.6913	−0.2371	2005:093	2012:049	6.9
P012	−1664,354.0682	−4743,667.0060	3915,064.0020	−0.5094	0.4920	−0.6833	2006:062	2012:049	6.0
P015	−1806,151.8248	−4959,806.5536	3571,755.7835	−0.6041	0.4992	−0.0628	2005:090	2012:049	6.9
P030	−1670,489.9362	−4464,885.0018	4226,344.1251	−0.0773	0.2189	−0.7995	2005:253	2012:049	6.4
P032	−1414,311.8573	−4553,166.4077	4225,680.8606	0.2990	0.7879	−1.3063	2005:341	2012:049	6.2
P033	−1374,663.6605	−4389,900.5305	4405,280.4562	0.4274	−0.6210	−0.9170	2005:339	2012:049	6.2
P034	−1483,356.0781	−5020,831.1881	3633,960.6655	−0.1339	0.1546	−0.0423	2004:142	2012:049	7.7
P035	−1376,910.5056	−5073,611.2080	3602,566.9090	−0.2453	0.3525	0.0656	2005:063	2012:049	7.0
P037	−1304,151.8852	−4831,831.3905	3943,232.9983	−0.1251	0.1912	−0.3970	2004:155	2012:049	7.7
P038	−1225,471.8105	−5141,071.4424	3560,657.2652	−0.6902	−1.2836	0.8944	2005:064	2012:049	7.0
P039	−1169,204.4276	−5003,010.6380	3769,191.9152	−0.4526	−0.7480	0.8111	2005:063	2012:049	7.0
*P040	−1104,361.4468	−4905,636.2687	3912,374.6683	−0.2647	−0.1151	0.1843	2005:349	2012:049	6.2
P041	−1283,634.1477	−4726,427.8722	4074,798.0317	−0.2010	0.0892	−0.5702	2004:053	2012:049	8.0
P042	−1220,743.5867	−4584,480.0868	4250,806.4004	0.2117	1.0156	−1.6274	2004:315	2012:049	7.3
*P044	−1116,560.2622	−4752,090.2737	4093,489.7112	0.0002	0.6023	−0.7610	2004:317	2012:049	7.3
P050	−152,5480.0224	−3923,083.4209	4777,585.2416	0.9494	−0.5808	−1.9124	2006:053	2012:049	6.0
P072	−2217,511.9696	−4401,202.9508	4038,453.0083	−2.4936	1.6186	−0.2953	2005:172	2012:049	6.7
P081	−2007,173.8209	−4535,571.6732	3999,122.1466	−2.6145	1.1567	−0.6809	2006:104	2012:049	5.8
P082	−1972,446.7314	−4535,189.6532	4016,349.9355	−2.5061	1.0298	−0.8616	2006:130	2012:049	5.8
P084	−1902,527.0521	−4470,353.4620	4120,779.6701	−2.6110	0.7140	−0.9229	2006:138	2012:049	5.8
P104	−1912,133.6652	−4567,268.9560	4009,233.5830	−1.9399	1.4215	−0.9858	2006:159	2012:049	5.7
P106	−1868,594.8211	−4564,647.5768	4032,777.4819	−2.2080	1.1881	−0.8168	2006:102	2012:049	5.9
P107	−1603,783.9379	−4971,337.3045	3651,015.6656	−0.4772	0.3733	−0.1813	2006:061	2012:049	6.0
P113	−1914,893.0086	−4451,028.3842	4135,665.1010	−2.6699	0.5736	−0.7030	2006:107	2012:049	5.8
P123	−1405,300.3417	−4929,803.0052	3786,420.6211	−0.6134	0.2608	−0.2719	2006:060	2012:049	6.0
P164	−2709,977.8126	−4064,463.8453	4088,860.3794	−6.1232	15.4659	11.3912	2004:223	2012:049	7.5
P171	−2705,141.3934	−4364,219.0205	3771,983.6236	−12.8131	32.9664	27.8973	2004:245	2012:049	7.5
P175	−2656,852.6019	−4398,263.1166	3766,589.6560	−13.4059	30.9563	27.6203	2006:139	2012:049	5.8
P181	−2697,940.9430	−4255,089.5310	3898,009.5575	−7.3187	22.9324	18.0298	2005:033	2012:049	7.0
P183	−2734,197.3389	−4199,233.1103	3932,827.2422	−6.7819	30.0040	24.8625	2006:154	2012:049	5.7
P213	−2694,809.2801	−4314,131.7219	3835,348.5971	−9.1370	25.7128	21.6323	2005:148	2012:049	6.7
P217	−2672,525.5773	−4335,539.0904	3826,692.0791	−10.2928	20.3470	18.9169	2005:090	2012:049	6.9
P222	−2689,640.1601	−4290,437.4694	3865,050.8666	−9.3572	22.7982	18.6028	2005:069	2012:049	6.9
P225	−2681,518.7271	−4281,621.8629	3880,440.3623	−7.3272	17.2086	13.4187	2005:022	2012:049	7.1
P240	−2667,666.3634	−4346,076.1102	3818,100.4830	−9.0292	21.6430	17.4587	2005:147	2012:049	6.7
P247	−2656,446.3424	−4388,313.7255	3778,580.5491	−13.1783	30.9762	27.1086	2006:147	2012:049	5.7
P262	−2673,021.8390	−4261,799.2094	3907,637.9366	−6.2342	14.7394	10.6935	2005:088	2012:049	6.9
P283	−2611,762.6519	−4472,137.8075	3711,069.8408	−6.2013	15.2933	15.7009	2006:152	2012:049	5.7
P285	−2645,512.0058	−4406,096.6554	3766,021.1482	−5.4429	11.2198	10.7735	2006:193	2012:049	5.6
P294	−2613,400.9907	−4447,338.6915	3739,546.0474	−4.0289	10.1085	10.7877	2006:138	2012:049	5.8
P295	−2658,829.0009	−4452,735.2665	3701,287.9416	−14.0538	29.4954	26.3494	2004:127	2012:049	7.8
P406	−2462,331.5966	−3769,689.1878	4502,302.9895	6.4034	1.1807	4.1712	2006:001	2012:049	6.1
P464	−2373,746.3226	−4577,465.3632	3742,992.4811	−3.4538	5.1001	3.5438	2006:074	2012:049	5.9
P470	−2422,555.2736	−4674,803.3596	3589,415.1097	−8.0271	12.9604	11.8789	2004:350	2012:049	7.2
P471	−2460,056.6583	−4717,507.0887	3506,174.6565	−16.0277	24.7174	22.1629	2006:011	2012:049	6.1
P515	−2638,414.1019	−4526,005.8277	3626,260.1169	−16.2173	30.4050	25.9723	2006:131	2012:049	5.8
P516	−2642,150.9150	−4506,429.8947	3647,663.0881	−13.9650	29.9237	26.8690	2006:036	2012:049	6.0
P523	−2672,969.4088	−4473,242.5486	3665,507.3237	−13.8401	31.5837	28.8606	2006:032	2012:049	6.0
P530	−2632,938.4809	−4473,335.4093	3694,658.2036	−11.5007	29.0563	25.0925	2005:189	2012:049	6.6
P532	−2616,024.4074	−4482,709.7801	3695,555.2699	−11.2525	23.3895	22.1778	2004:282	2012:049	7.4
P536	−2608,523.7088	−4513,542.9494	3663,632.6476	−13.2194	24.7357	22.3684	2006:125	2012:049	5.8
P537	−2600,237.1712	−4515,503.8487	3666,937.5790	−12.1433	22.0964	20.3637	2006:124	2012:049	5.8
P538	−2607,196.7000	−4495,390.0135	3686,626.6574	−11.7818	21.3642	20.1339	2006:125	2012:049	5.8
P539	−2607,160.9029	−4482,780.8762	3701,802.5649	−8.1512	16.6641	16.1847	2005:091	2012:049	6.9
P540	−2599,843.6746	−4479,443.8494	3710,561.0770	−6.1692	13.8289	12.4002	2006:038	2012:049	6.0

Table B1 (*Continued*)

Station	Position at epoch 2005.0 (m)			Velocity (mm/a)			Start epoch (year:day)	Stop epoch (year:day)	Span (yr)
*Core	*X*	*Y*	*Z*	*X*	*Y*	*Z*			
P541	−2593,314.3662	−4491,629.6557	3700,137.3038	−6.9343	13.2511	13.1009	2005:188	2012:049	6.6
P543	−2582,627.2660	−4525,401.1114	3667,114.6240	−9.1414	15.7924	15.6318	2006:172	2012:049	5.7
P556	−2506,664.2877	−4607,980.2916	3617,523.4612	−8.7862	16.1363	14.1294	2005:309	2012:049	6.3
P557	−2510,627.3359	−4594,205.7071	3633,852.4734	−8.2834	12.7251	12.5594	2005:253	2012:049	6.4
P558	−2501,018.5299	−4584,973.3691	3651,264.7892	−7.4067	11.7215	10.6266	2006:200	2012:049	5.6
P559	−2510,437.4349	−4601,105.1397	3623,743.2136	−8.1999	14.7156	13.4740	2005:309	2012:049	6.3
P560	−2504,755.9688	−4605,350.4349	3622,134.8651	−8.4265	13.7352	14.1236	2005:077	2012:049	6.9
P562	−2471,753.8188	−4611,976.8383	3636,954.5409	−4.9451	12.0381	11.2277	2004:233	2012:049	7.5
P579	−2455,163.2126	−4616,370.0015	3641,867.6219	−3.8841	11.5920	10.3662	2006:165	2012:049	5.7
P581	−2448,465.0525	−4657,908.8201	3593,733.3267	−8.5703	14.7995	13.0466	2005:350	2012:049	6.2
P583	−2419,314.4530	−4638,878.8606	3637,104.7437	−3.8422	10.6019	9.2849	2005:308	2012:049	6.3
P584	−2402,400.3273	−4724,830.6757	3536,976.1973	−10.4385	15.5874	17.0341	2004:143	2010:094	5.9
P588	−2402,809.5502	−4661,824.8163	3618,747.7992	−5.0569	10.4841	9.1787	2005:027	2012:049	7.1
P589	−2394,900.1680	−4677,993.7884	3603,967.8591	−6.3950	10.8481	10.0831	2005:015	2010:094	5.2
P591	−2452,571.9550	−4609,419.2605	3652,114.1861	−3.8224	10.8529	9.8844	2005:178	2012:049	6.6
P594	−2380,046.1590	−4593,510.6346	3719,463.3128	−4.1569	6.0924	4.6197	2005:022	2012:049	7.1
P595	−2386,904.4568	−4604,247.9094	3701,367.0788	−3.6736	7.5150	5.3425	2005:295	2012:049	6.3
P722	−1501,536.8951	−4223,566.6023	4524,171.1764	0.8127	0.1167	−1.7246	2005:281	2012:049	6.4
PARL	1257,781.1936	−4713,813.3986	4094,697.1822	−0.2423	0.7251	−1.0583	2003:127	2012:049	8.8
*PBCH	967,386.3324	−5611,812.2622	2863,022.8430	0.0258	−0.5092	0.3006	2005:026	2012:049	7.1
PBPP	−2464,204.6723	−4649,642.6618	3593,554.9526	−10.5383	16.5894	14.3675	2001:115	2012:049	10.8
PCK1	435,551.3360	−4411,842.1292	4570,400.1649	0.2393	−2.4703	0.2759	2003:001	2008:130	5.4
PDBG	−1528,846.9781	−5055,234.4454	3566,697.6640	0.2777	−1.5970	0.8269	2005:324	2012:049	6.2
PERL	−2293,867.0217	−4563,550.9194	3809,496.7126	−2.4150	1.7744	0.4657	2000:001	2011:206	11.6
PHLB	−2433,417.1285	−4636,062.1630	3631,593.8364	−4.4630	11.8013	10.2035	2000:025	2012:049	12.1
PIE1	−1640,916.9011	−5014,781.1976	3575,447.0960	−0.8640	0.1010	0.2770	1999:153	2012:049	12.7
POIN	−2257,895.8497	−4604,901.9590	3780,581.5981	−2.1075	1.4474	0.0081	1999:336	2011:103	11.4
PSC1	1238,380.8769	−4390,853.3005	4443,024.6378	0.0580	−1.6132	0.2155	2001:075	2012:036	10.9
PSU1	1017,619.5600	−4726,563.0036	4146,418.8316	−0.5476	0.7967	−0.7242	1998:033	2012:049	14.0
PTIR	411,673.7266	−4380,216.7803	4602,610.3353	−0.4512	−2.3758	0.0515	2003:105	2012:049	8.8
PVHS	−2521,923.7822	−4669,621.6289	3526,283.7679	−16.3170	27.5241	23.8052	1999:188	2012:049	12.6
PWEL	870,505.2246	−4571,872.9451	4346,729.0838	−0.3925	−0.3077	−0.7398	2002:160	2012:049	9.7
QCY2	−2665,893.1327	−4412,795.8281	3742,695.3489	−13.3990	31.1505	27.0285	2006:137	2012:049	5.8
RAIL	−2171,785.1774	−4519,731.8557	3930,901.7888	−2.4570	1.3765	−0.5580	1999:312	2011:204	11.7
RCA2	−2609,202.3229	−4570,711.5933	3592,958.0580	−18.1267	28.0205	24.0879	2000:271	2012:049	11.4
RELA	−2288,699.9389	−4579,550.1290	3792,622.1765	−2.3997	1.6480	0.4128	2000:001	2010:024	10.1
ROCK	−2533,220.1187	−4631,543.4800	3568,400.4932	−15.4222	26.0790	23.0131	1996:001	2012:049	16.1
RSTP	−2475,098.7468	−4617,408.6979	3626,913.5788	−5.6882	13.3225	11.9210	1999:181	2012:049	12.6
RUBY	−2059,032.6309	−4391,007.6412	4131,473.4502	−2.5189	1.4700	-0.8425	1999:198	2012:049	12.6
SA11	−1295,968.2750	−4620,523.4280	4190,675.0121	−0.7401	0.8667	-1.2114	2004:147	2012:049	7.7
SASK	−1106,129.6944	−3758,704.8893	5016,675.5195	−0.0274	−1.4297	−1.7346	2003:129	2012:049	8.8
SBCC	−2470,209.0830	−4712,749.6126	3505,283.6975	−16.1028	26.1679	22.4207	1999:313	2012:049	12.3
SC01	−1543,918.7164	−5060,497.7206	3553,867.8769	−0.9005	−1.2809	−0.0420	2001:267	2012:049	10.4
SCIA	−2417,842.1039	−4666,822.4159	3602,580.8311	−6.8685	12.3346	10.8881	2000:251	2012:049	11.4
SDHL	−2336,821.6009	−4732,586.7484	3570,332.3295	−2.3503	4.5253	6.8931	2001:353	2010:094	8.3
*SG01	−667,800.8964	−5082861.1424	3782390.9790	−0.1408	0.2622	0.0158	2001:175	2012:049	10.7
*SG04	−643,953.8053	−5050,568.7999	3829,291.8974	−0.2877	0.1675	0.0403	2001:254	2011:093	9.6
*SG05	917,687.8144	−5557,048.6897	2982,882.3640	0.2305	0.5775	−0.1351	2002:036	2012:049	10.0
SG07	1646,124.7519	−4215,280.3793	4479,662.5414	0.1096	−0.5516	−0.2759	2001:298	2008:224	6.8
*SG09	−740,324.6030	−5084,458.5501	3766,986.8409	−0.0744	0.4253	−0.5550	2001:261	2010:258	9.0
SG12	−812,558.1350	−4952,858.0415	3923,462.2759	0.1651	0.4163	−0.6350	2001:305	2009:287	8.0
*SG15	−489,205.5290	−4994,912.8676	3923,307.6701	−0.1211	0.4685	−0.5606	2001:319	2009:301	8.0
SG23	258,990.2039	−4854,551.0989	4115,216.0153	−0.2753	1.2038	−1.3056	2002:199	2010:274	8.2
SG33	−1542,318.7942	−5204,676.9112	3339,687.2065	−0.1435	−0.1183	0.2653	2004:009	2012:049	8.1
SG34	−611,895.7576	−5177,440.0156	3662,438.1091	−0.1727	−1.0904	0.0185	2003:170	2009:334	6.5
SGDM	−2467,931.8376	−4668,655.8830	3565,569.8187	−15.0026	21.0241	17.1090	2003:214	2012:047	8.5
SHLD	−2307,792.9263	−4160,682.2005	4235,700.1215	−2.2871	1.8849	1.6150	1999:303	2007:273	7.9
SHOS	−2289,859.6734	−4633,385.7613	3725,961.0745	−2.5968	1.6639	0.7531	2000:001	2010:094	10.3
SIBY	557,185.5017	−4701,542.8179	4259,733.4518	−0.4857	0.8712	−1.3985	2002:152	2012:049	9.7
SKUL	−2260,889.4249	−4592,584.0189	3794,201.4985	−2.2216	1.6498	−0.0538	2000:001	2010:354	11.0
SLAC	−2703,115.9336	−4291,767.2168	3854,247.8758	−10.1146	26.0129	21.4480	2003:032	2011:032	8.0
*SNFD	978,158.1752	−5107,368.3443	3680,831.1673	−0.1813	−0.0372	−0.0913	2002:104	2012:049	9.8
SNHS	−248,1345.1263	−4680,788.7736	3539,798.7860	−15.5046	24.5312	21.1317	1999:148	2012:049	12.7
STJO	2612,631.0913	−3426,807.0376	4686,757.8779	−1.3287	0.1269	0.7288	1996:001	2012:049	16.1
STRI	−2273,528.5129	−4592,506.5144	3786,437.9753	−2.2179	1.4988	0.2810	2000:001	2011:102	11.3
SUP2	227,623.1358	−4452,600.4323	4545,971.4778	−0.2097	−1.0217	−1.1515	2001:246	2012:049	10.5
SUP3	345,351.5831	−4400,681.0263	4588,713.7875	−0.3818	−2.5060	−1.4638	2001:246	2012:049	10.5
TATE	−2284,024.4977	−4566,211.3554	3812,106.6751	−2.2816	1.6132	0.2860	2000:001	2011:102	11.3
THCP	−2484,731.2352	−4592,622.3689	3653,179.8563	−6.4889	11.2673	10.0226	2000:342	2012:049	11.2
THU3	538,093.5456	−1389,088.0446	6180,979.2386	−1.8872	−4.5782	6.2757	2002:145	2012:049	9.7
TIVA	−2256,689.2784	−4580,202.2753	3812,838.7297	−2.3293	1.4229	0.0642	2000:001	2010:024	10.1
TOIY	−2240,595.5597	−4388,057.9405	4040,379.0737	−2.7524	1.3542	0.0620	2003:038	2012:049	9.0
TONO	−2296,771.2751	−4472,097.2069	3915,214.3534	−2.5646	1.9116	0.1779	1999:355	2012:049	12.2
TORP	−2517,894.4485	−4670,259.9728	3527,827.5781	−16.2375	26.9831	23.5478	1997:059	2012:049	15.0

Table B1 (*Continued*)

Station	Position at epoch 2005.0 (m)			Velocity (mm/a)			Start epoch (year:day)	Stop epoch (year:day)	Span (yr)
*Core	*X*	*Y*	*Z*	*X*	*Y*	*Z*			
TUNG	−2303,207.6432	−4285,131.6967	4113,097.4965	−3.5689	2.9794	1.1056	1996:203	2012:049	15.6
*TXCH	−939,437.9740	−5180,555.8412	3588,916.9011	0.6877	0.1514	−0.0544	2005:025	2012:049	7.1
*TXLL	−828,003.6728	−5424,581.8001	3240,692.2769	0.3261	0.1527	0.4666	2005:211	2012:049	6.6
TXMA	−402,504.0053	−5367,362.0786	3410,668.3373	0.1877	1.1552	0.4842	2005:211	2012:049	6.6
*TXSN	−1186,342.6303	−5391,538.5203	3185,437.6746	0.2039	−0.1951	0.2377	2005:211	2012:049	6.6
UNIV	462,323.5302	−4703,239.1211	4269,305.4734	−0.3561	0.4860	−1.1364	2001:255	2012:049	10.4
UOFM	507,058.0969	−4697,843.2255	4270,129.3552	0.0052	1.3434	−1.0190	2005:091	2012:049	6.9
UPSA	−2370,479.9739	−4311,480.7946	4046,969.9136	−3.9132	3.9756	1.8493	1999:236	2012:049	12.5
UPTC	856,680.4821	−4697,260.5756	4215,103.9144	−0.2967	0.1163	−1.1141	2000:265	2012:049	11.4
*USNO	1112,189.7728	−4842,955.0266	3985,352.2660	−0.4160	0.6589	−0.7307	1997:121	2012:049	14.8
VALD	919,075.8040	−4167,766.2479	4724,323.5443	1.1867	−7.1300	5.5243	2003:063	2012:049	9.0
*VALY	957,347.4498	−4983,885.7458	3850,753.9945	−0.3450	0.0598	−0.0701	2004:134	2011:252	7.3
*VAST	954,103.0195	−4930,281.3130	3919,710.2340	−0.3238	−0.2101	0.0953	2003:219	2011:239	8.1
VIMT	−2523,363.0902	−4644,670.2082	3558,376.5825	−16.4376	25.7571	22.4048	2000:194	2012:049	11.6
VNCX	−2515,892.3602	−4636,680.6738	3573,547.3274	−15.8870	23.3543	19.9782	1998:364	2012:049	13.1
VTIS	−2517,409.1160	−4676,544.1057	3520,010.2619	−16.2739	27.7273	23.9894	1998:343	2012:049	13.2
VTUV	1317,909.9752	−4364,546.2795	4445,527.1666	−0.2706	−1.2041	−0.0094	2004:336	2012:049	7.2
WARR	572,003.6134	−4672,334.9554	4289,606.7524	−0.6143	0.5089	−1.3777	2004:356	2012:049	7.2
WHYT	−2465,333.1506	−4707,048.6273	3516,603.8251	−15.5353	25.2559	22.1463	2001:172	2012:049	10.7
WRUN	531,992.0288	−4699,633.7274	4265,072.7739	−0.5540	0.7363	−1.2548	2004:356	2012:049	7.2
*XCTY	665,804.9642	−5508,488.6581	3134,878.0670	−0.0692	−0.0803	−0.1966	2004:042	2012:049	8.0
YELL	−1224,452.6635	−2689,216.1391	5633,638.2813	−2.1536	−5.1664	4.7379	1996:235	2012:049	15.5
YORK	1122,458.5384	−4763,241.5644	4076,945.4595	−0.2275	1.0328	−0.8100	2002:242	2012:049	9.5
*ZEFR	766,680.6613	−5571,328.4301	2998,751.0198	−0.2339	0.3108	−0.3033	2003:246	2012:049	8.5

References

Akaike, H., 1974. A new look at the statistical model identification. IEEE Trans. Autom. Control AC-19 (6), 716–723.

Altamimi, Z., Collilieux, X., Métivier, L., 2011. ITRF2008: an improved solution of the international terrestrial reference frame. J. Geod. 85, 457–473, http://dx.doi.org/10.1007/s00190-011-0444-4.

Altamimi, Z., Collilieux, X., Métivier, L., 2012. ITRF2008 plate motion model. J. Geophys. Res. 117 (B7), http://dx.doi.org/10.1029/2011JB008930, B07402.

Argus, D.F., Gordon, R.G., Heflin, M.B., Ma, C., Eanes, R.J., Willis, P., Peltier, W.R., Owen, S.E., 2010. The angular velocities of the plates and the velocity of the Earth's centre from space geodesy. Geophys. J. Int. 18, 1–48, http://dx.doi.org/10.1111/j.1365-246X.2009.04463.x.

Argus, D.F., Peltier, W.R., 2010. Constraining models of postglacial rebound using space geodesy: a detailed assessment of model ICE-5G (VM2) and its relatives. Geophys. J. Int. 181 (2), 697–723, http://dx.doi.org/10.1111/j.1365-246X.2010.04562.x.

Bar Sever, Y.E., Kroger, P.M., Borjesson, J.A., 1998. Estimating horizontal gradients of tropospheric path delay with a single GPS receiver. J. Geophys. Res. Solid Earth 103, 5019–5035, http://dx.doi.org/10.1029/97JB03534.

Berglund, H.T., Sheehan, A.F., Murray, M.H., Roy, M., Lowry, A.R., Nerem, R.S., Blume, F., 2012. Distributed deformation across the Rio Grande Rift Great Plains, and Colorado Plateau. Geology 40 (1), 23–26, http://dx.doi.org/10.1130/G32418.1.

Bertiger, W., Desai, S.D., Haines, B., Harvey, N., Moore, A.W., Owen, S., Weiss, J.P., 2010. Single receiver phase ambiguity resolution with GPS data. J. Geod. 84 (5), 327–337, http://dx.doi.org/10.1007/s00190-010-0371-9.

Blewitt, G., 2007. GPS and space based geodetic methods. In: Herring, T., Schubert, G. (Eds.), Treatise on Geophysics, 3. Academic Press, Oxford, UK, ISBN 0-444-51928-9, pp. 351–390.

Blewitt, G., 2003. Self-consistency in reference frames, geocenter definition, and surface loading of the solid Earth. J. Geophys. Res. 108 (B2), 210, http://dx.doi.org/10.1029/2002JB002082.

Blewitt, G., Lavallée, D., 2002. Effect of annual signals on geodetic velocity. J. Geophys. Res. 107 (B7), http://dx.doi.org/10.1029/2001JB000570.

Blewitt, G., 1998. GPS data processing methodology: from theory to applications. In: Teunissen, P.J.G., Kleusberg, A. (Eds.), GPS for Geodesy. Springer-Verlag, Berlin, pp. 231–270, ISBN: 3-540-63661-7.

Blewitt, G., Heflin, M.B., Webb, F.H., Lindqwister, U.J., Malla, R.P., 1992. Global coordinates with centimeter accuracy in the International Terrestrial Reference Frame using the Global Positioning System. Geophys. Res. Lett. 19, 853–856.

Blewitt, G., 1990. An automatic editing algorithm for GPS data. Geophys. Res. Lett. 17 (3), 199–202.

Blewitt, G., 1989. Carrier phase ambiguity resolution for the Global Positioning System applied to geodetic baselines up to 2000 km. J. Geophys. Res. 94 (B8), 10187–10283.

Boehm, J., Niell, A., Tregoning, P., Schuh, H., 2006. Global mapping function (GMF): a new empirical mapping function based on numerical weather model data. Geophys. Res. Lett. 33 (L07304), http://dx.doi.org/10.1029/2005GL025546.

Calais, E., Mattioli, G.S., DeMets, C., Nocquet, J., Stein, S., Newman, A., Rydelek, P., 2005. Seismology: tectonic strain in plate interiors? Nature 438 (7070), E9–E10, http://dx.doi.org/10.1038/nature04428.

Calais, E., Han, J.Y., DeMets, C., Nocquet, J.M., 2006. Deformation of the North American plate interior from a decade of continuous GPS measurements. J. Geophys. Res. 111 (B6), http://dx.doi.org/10.1029/2005JB004253, B06402.

DeMets, C., Gordon, R.G., Argus, D.F., 2010. Geologically current plate motions. Geophys. J. Int. 181, 1–80, http://dx.doi.org/10.1111/j.1365-246X.;1;2009.04491.x, See also Erratum.

DeMets, C., Gordon, R.G., Argus, D.F., Stein, S., 1994. Effect of recent revisions to the geomagnetic reversal time scale on estimates of current plate motions. Geophys. Res. Lett. 21, 2191–2194.

Fu, Y., Freymueller, J.T., van Dam, T., 2011. The effect of using inconsistent ocean tidal loading models on GPS coordinate solutions. J. Geod. 86 (6), 409–421, http://dx.doi.org/10.1007/s00190-011-0528-1.

Herring, T., Craymer, M., Sella, G., Snay, R., Blewitt, G., Argus, D., Bock, Y., Calais, E., Davis, J., Tamisiea, M., 2008. SNARF 2.0: a regional reference frame for North America. Eos Trans. AGU 89 (23), Jt. Assemb. Suppl., Abstract G31B-01.

Koch, K.-R., 1999. Parameter Estimation and Hypothesis Testing in Linear Models, second ed. Springer, Berlin, Heidelberg.

Kreemer, C., Blewitt, G., Bennett, R.A., 2010a. Present-day motion and deformation of the Colorado Plateau. Geophys. Res. Lett. 37 (10), http://dx.doi.org/10.1029/2010GL043374, L10311.

Kreemer, C., Gordon, R.G., Mishra, J.K., 2010b. The effect of horizontal thermal contraction on oceanic intraplate deformation: examples for the Pacific. Geophys. Res. Abstr. 12, EGU2010–EGU13104.

Kumar, R.R., Gordon, R.G., 2009. Horizontal thermal contraction of oceanic lithosphere: the ultimate limit to the rigid plate approximation. J. Geophys. Res. Solid Earth 114 (B1), http://dx.doi.org/10.1029/2007JB005473, B01403.

McCaffrey, R., 2005. Block kinematics of the Pacific–North America plate boundary in the southwestern United States from inversion of GPS, seismological and geologic data. J. Geophys. Res. 110, http://dx.doi.org/10.1029/2004JB002207, B07401.

Meade, B.J., Hager, B.H., 2005. Block models of crustal motion in southern California constrained by GPS measurements. J. Geophys. Res. 110, http://dx.doi.org/10.1029/2004JB003209, B03403.

Peltier, W.R., Drummond, R., 2008. Rheological stratification of the lithosphere: a direct inference based on the geodetically observed pattern of the glacial isostatic adjustment of the North American continent. Geophys. Res. Lett. 35 (L16314), http://dx.doi.org/10.1029/2008GL034586.

Petit, G., Luzum, B., 2010. IERS Conventions (2010). In: IERS Technical Note 36. Frankfurt am Main., pp. 179, ISBN: 3-89888-989-6.

Rebischung, P., Griffiths, J., Ray, J., Schmid, R., Collieux, X., Garayt, B., 2012. IGS08: the IGS realization of ITRF2008. GPS Sol. 16 (4), 483–494.

Scherneck, H.-G., 1991. A parametrized solid earth tide model and ocean tide loading effects for global geodetic baseline measurements. Geophys. J. Int. 106 (3), 677–694, http://dx.doi.org/10.1111/j.1365-246X.1991.tb06339.x.

Sella, G.F., Stein, S., Dixon, T.H., Craymer, M., James, T.S., Mazzotti, S., Dokka, R.K., 2007. Observation of glacial isostatic adjustment in "stable" North America with GPS. Geophys. Res. Lett. 34, http://dx.doi.org/10.1029/2006GL027081, L02306.

Schmid, R., Steigenberger, P., Gendt, G., Ge, M., Rothacher, M., 2007. Generation of a consistent absolute phase center correction model for GPS receiver and

satellite antennas. J. Geod. 81 (12), 781–798, http://dx.doi.org/10.1007/s00190-007-0148-y.

Wdowinski, S., Bock, Y., Zhang, J., Fang, P., Genrich, J., 1997. Southern California permanent GPS geodetic array: spatial filtering of daily positions for estimating coseismic and postseismic displacements induced by the 1992 Landers earthquake. J. Geophys. Res. 102, 18057–18070.

Wessel, P., Smith, W.H.F., 1998. New, improved version of generic mapping tools released. EOS Trans. Am. Geophys. Union 79 (47), 579.

Zumberge, J.F., Heflin, M.B., Jefferson, D.C., Watkins, M.M., Webb, F.H., 1997. Precise point positioning for the efficient and robust analysis of GPS data from large networks. J. Geophys. Res. 102 (B3), 5005–5017.